RNAi Screen Identifies KIF15 as a Novel Regulator of Integrin Endocytic Trafficking

running title: KIF15 regulates integrin endocytosis

Anastasia Eskova[1], Bettina Knapp[2], Dorota Matelska[1], Susanne Reusing[1], Antti Arjonen[3], Tautvydas Lisauskas[1], Rainer Pepperkok[4], Robert Russell[1], Roland Eils[1,5], Johanna Ivaska[3], Lars Kaderali[2], Holger Erfle[1], and Vytaute Starkuviene*[1]

*Corresponding author

Mailing address:
Vytaute Starkuviene
BioQuant
Ruprecht-Karls-University Heidelberg
Im Neuenheimer Feld 267
69120 Heidelberg
Tel: (+49) 06221 54 51295
Fax: (+49) 06221 54 51483
e-mail: vytaute.starkuviene@bioquant.uni-heidelberg.de

Affiliations

[1]BioQuant, University of Heidelberg, 69120 Heidelberg, Germany

[2]Medical Faculty, Institute for Medical Informatics and Biometry (IMB), Technische Universität Dresden, 01307 Dresden, Germany

[3]Centre for Biotechnology, University of Turku, 20520 Turku, Finland

[4]EMBL, Meyerhofstraße 1, 69117 Heidelberg, Germany

[5]Integrative Bioinformatics and Systems Biology, DKFZ, BioQuant and Institute of Pharmacy and Molecular Biotechnology, University of Heidelberg, 69120 Heidelberg, Germany

Keywords
Integrin / endocytic trafficking / KIF15 / Dab2

JCS Advance Online Article. Posted on 21 March 2014

Summary

α2β1 integrin is one of the most important collagen-binding receptors and has been implicated in numerous widely spread thrombotic and immune diseases. α2β1 integrin is a potent tumour suppressor and its downregulation is associated with increased metastasis and poor prognosis in breast cancer. Currently, very little is known about the mechanism regulating α2β1 integrin cell surface expression and trafficking. Here, using a quantitative fluorescent microscopy-based RNAi assay, we investigated the impact of 386 cytoskeleton-associated or regulatory genes on α2-integrin endocytosis and scored 122 hits affecting α2-integrin intracellular accumulation. Of these, 83 were identified to be putative regulators of α2-integrin trafficking and/or expression with no observed effect on EGF or transferrin internalization. Further interrogation and validation of the siRNA screen revealed a role for KIF15, a microtubule-based molecular motor, as a significant inhibitor of α2-integrin endocytic trafficking. Our data suggest a novel role for KIF15 in mediating plasma membrane localization of the alternative clathrin adaptor Dab2, thus impinging on pathways regulating α2-integrin internalization.

Introduction

Integrins are one of the major cell surface adhesion receptors, involved in numerous functions, such as cell migration, signal transduction, proliferation, survival and differentiation. Currently, 18 integrin α and 8 β chains are known in human cells, forming 24 different heterocomplexes specific for diverse ligands (Takada et al., 2007, Humphries et al., 2006, Caswell et al., 2009). Availability and functionality of integrins on the cell surface strongly depends on their biosynthetic trafficking, internalization, recycling and degradation (Margadant et al., 2011).

Newly synthesized integrins are assembled into heterodimers in the endoplasmic reticulum (Heino et al., 1989, Huang et al., 1997), traverse the Golgi complex in the inactive state (Tiwari et al., 2011) and require binding to TGN38/46 at the *trans*-Golgi to efficiently reach the plasma membrane (PM) (Wang and Howell, 2000). Both ligand-bound (clustered) and non-bound (non-clustered) surface integrins can be internalized (Valdembri et al., 2011, Arjonen et al., 2012) and clathrin-dependent and clathrin-independent pathways have been elucidated for the internalisation of different integrins (Caswell et al., 2009). Unlike many other endocytic cargoes, integrin internalization via the clathrin-dependent pathway often requires clathrin-associated sorting proteins CLASPs (for instance, Dab2, Numb or ARH) (Nishimura and Kaibuchi, 2007, Ezratty et al., 2009, Tackchandani et al., 2009). The majority of the internalized integrins are recycled back to the PM

(Caswell and Norman, 2006) either through Rab11- (long-loop) or Rab4- (short-loop) specific pathways (Roberts et al., 2001, Powelka et al., 2004, Arjonen et al., 2012). Ligand-bound integrins can also be directed to lysosomal or non-lysosomal degradation pathways (Arjonen et al., 2012, Valdembri et al., 2009, Rintanen et al., 2012, Lobert et al., 2010, Tiwari et al., 2011, Dozynkiewicz et al., 2012). Competitive binding of diverse regulators to integrins may promote recycling or intracellular retention (Mai et al., 2011, Böttcher et al., 2012). The exact pathway of integrin trafficking depends not only on the integrin activation state, but also on cell type, composition of the integrin heterodimer, trafficking of other integrins and extracellular stimuli (Caswell and Norman, 2006).

Despite the complexity of trafficking pathways, regulators involved in integrin internalization, recycling or degradation are emerging. Small GTPases of the Rab family (Rab4, Rab5, Rab7, Rab11, Rab21, Rab25) are critical regulators of endocytic integrin trafficking (Roberts et al., 2001, Powelka et al., 2004, Arjonen et al., 2012, Pellinen et al., 2006, Caswell et al., 2007) and diverse SNAREs, mediators of membrane fusion, have been described for integrin recycling (e.g., SNAP23-syntaxin 4-VAMP3 complex, syntaxin 3, syntaxin 6) (Skalski et al., 2010, Veale et al., 2010, Tiwari et al., 2011, Day et al., 2011). In addition, several molecular motors play a role in integrin trafficking. For instance, actin-based motors, such as myosin 10, regulate integrin-mediated cell adhesion in filopodia (Zhang et al., 2004), and myosin 6 promotes internalization of ligand-bound α5β1 integrin (Valdembri et al., 2009). Microtubule-based motor KIF1C promotes delivery of α5β1 integrin from the perinuclear recycling compartment to the trailing edge of migrating cells (Theisen et al., 2012). However, a comprehensive characterization of the molecular machinery regulating integrin trafficking is still missing.

β1-integrin is frequently used to investigate integrin trafficking; however, it forms heterodimers with 12 different α chains (Hynes, 2002). As different heterodimers exhibit different trafficking kinetics (Caswell et al., 2009) and may have different molecular requirements (Teckchandani et al., 2009) analysis of the selected α chain may be more advantageous in delineating specific molecular mechanisms. α2-integrin interacts only with the β1 integrin subunit (Hynes, 1992), and α2β1 heterodimer is expressed in fibroblasts, keratinocytes, leukocytes, epithelial and endothelial cells, and platelets. Being one of the most important receptor of collagen (Kramer and Marks, 1989, Hemler et al., 1990, Emsley et al., 2000), α2β1 is crucial for haemostasis, morphogenesis of tubular organs, angiogenesis, platelet aggregation, renewal of the epidermis and wound healing (Chen et al., 2002, Eble, 2005). It is also involved in numerous thrombotic and immune diseases (Eckes et al., 2000, Santoro, 1999, De Fougerolles et al., 2000).

Importantly, expression of integrin α2β1 is strongly reduced in breast cancer and α2β1 downregulation correlates with increased cell invasion and metastasis and thus poor prognosis (Zutter et al., 1998 Ramirez et al., 2011). Integrin α2β1 also acts as a co-receptor for several pathogens, such as EV1, rotavirus and HCMV (Bergelson et al., 1992, Londrigan et al., 2003, Feire et al., 2004, Fleming et al., 2010). Binding of EV1 induces clustering of inactive α2β1 and directs virus-bound α2-integrin to a calpain-dependent degradation pathway in multivesicular bodies (Rintanen et al., 2012, Karjalainen et al., 2008, Upla et al., 2004). Binding of α2β1 to collagen may direct the heterodimer to the same degradation pathway (Rintanen et al., 2012). In contrast, little is known about the trafficking route of non-clustered α2β1 integrin, apart from a role for Rab21 binding to the α2-integrin cytoplasmic tail to facilitate endocytosis and binding of p120RasGAP that facilitates recycling to the PM (Mai et al., 2011).

Here, we used an unbiased quantitative fluorescence microscopy-based RNAi screen to identify regulators of α2-integrin endocytic trafficking. We targeted the expression of 386 chosen proteins that are functionally related to membrane trafficking and the cellular cytoskeleton. Of these, 122 were demonstrated to affect α2-integrin intracellular accumulation and half of these were novel regulators in the context of endocytosis. We chose to characterize in more details the role of one of the strongest validated inhibitors of α2-integrin trafficking, the molecular motor KIF15. Our data suggest novel regulation of α2-integrin internalization through motor-dependent PM localization of the alternative clathrin adaptor, Dab2.

Results

Endocytic trafficking of endogenous α2-integrin

To define whether α2-integrin undergoes heterodimer-specific endocytic trafficking, we compared the endocytosis of α2-integrin in HeLa cells (chosen due to ease of transfection, and good RNAi efficiency) with the previously characterized trafficking of β1-integrin. Cell surface α2-integrin was antibody-labelled at 4^{o}C for 1h and then internalized at 37^{o}C for varying time points on plastic dishes. In order to quantify the amount of intracellular α2-integrin, the remaining cell surface integrin-antibody complexes were removed by treating cells with an acidic buffer (see **Methods,** (Erfle et al., 2011)). Internalized α2-integrin accumulated efficiently at the juxtanuclear area and cytoplasmic structures (**Fig. 1A,D**) after 1h. α2-integrin localized largely to the scattered cytoplasmic structures after prolonged incubation time of 6h (**Fig. 1A**). There was a progressive reduction of cell surface α2-integrin (**Fig. 1B,E**), similar to levels measured for β1-integrin in

HeLa cells (Teckchandani et al., 2009). In contrast, antibody-clustered α2-integrin (see **Methods**), accumulated in cytoplasmic punctate structures with hardly any residual PM localization (**Fig. 1C**) as reported in (Rintanen et al., 2012, Karjalainen et al., 2008, Upla et al., 2004).

In order to determine the α2-integrin endocytic route following internalisation several GFP-Rab GTPases were overexpressed and cells were stained for α2-integrin. Similar to β1-integrin (Powelka et al., 2004, Arjonen et al. 2012), following 1h of internalization >70% of the intracellular α2-integrin co-localized to peripheral structures positive for overexpressed Rab5a GTPase (**Fig. 2A**). Only 10% of the peripheral α2-integrin-containing structures were Rab7a positive (**Fig. 2D)**, suggesting that, α2–integrin enters the Rab7a-dependent lysosomal degradation pathway inefficiently. Approximately 70% of the peripheral α2-integrin-containing structures were Rab11b and Rab4a positive (**Fig. 2B,C**) – a strong indication that α2-integrin enters short- and long-loop recycling pathways. Interestingly, unlike β1-integrin (Powelka et al., 2004), perinuclear localization of α2-integrin was reduced when Rab11b and Rab4a were overexpressed (**Fig. 2B,C**).

Previous RNAi experiments demonstrated that endocytosis of β1-integrin occurs via clathrin-dependent pathway in various cell types (Nishimura and Kaibuchi, 2007,12, Chao and Kunz, 2009) and by a caveolin-dependent pathway in myofibroblasts (Shi and Sottile, 2008). The latter pathway is also utilized by α2-integrin in ovarian carcinoma cells when EGFR is activated (Ning et al., 2007) or upon clustering of α2β1 integrin by antibodies (Upla et al., 2004), suggesting possible cell-type-specific mechanisms. To investigate whether both of these pathways play a role in α2-integrin endocytic trafficking in HeLa cells we depleted the key components of clathrin-dependent and caveolae-dependent pathways (clathrin heavy chain (CLTC), caveolin-1 (CAV1), and dynamin-2 (DNM2)) (Hansen and Nichols, 2009, Doherty and McMahon, 2009). The efficiency of the respective siRNAs was tested by western blot or immunofluorescence staining, and demonstrated a 50-80% reduction of the target proteins after 48 h of transfection (**Fig. S1**). Even not a complete reduction of CLTC, CAV1 or DNM2 expression was sufficient to inhibit intracellular accumulation of α2-integrin by 70-80% (**Fig. 1F,G**).

Potential regulators of α2-integrin intracellular accumulation identified by RNAi assays

To identify regulators of α2-integrin intracellular accumulation, we performed a fluorescent microscopy-based RNAi screen with 1084 siRNAs targeting 386 genes (**Table S1).** The targeted library (provided by Dr R. Pepperkok, EMBL) was designed to include most mammalian motor proteins: 44 kinesin heavy chains, 13 dynein subunits (the 3 major heavy chains and 10 cargo-binding light chains) and 37 myosins. In addition, proteins regulating membrane trafficking and/or

cytoskeletal dynamics were included based on literature data: 28 small Ras and Rho GTPases, 53 GAPs and 62 GEFs of these GTPases, 41 actin-associated and 14 microtubule-associated proteins, 34 kinases and 9 phosphatases, 5 different β–integrin chains, and 23 scaffold and adaptor proteins. For the primary screen we used pre-spotted Lab-Tek chambers with the siRNAs and Lipofectamine (reverse transfection on cell arrays (Erfle et al., 2007)). These were prepared in one spotting experiment, ensuring a high efficiency and reproducibility of the whole screen (see **Methods).** We quantified the α2-integrin-specific intracellular fluorescence signal for individual cells after 1 h of internalization when the level of intracellular α2-integrin was the highest in the control specimen (**Fig. 1D**), thereby, achieving the best signal-to-noise ratio during the screen. Inspection of the control samples over large cell populations revealed a large variation in the amount of internalized α2-integrin in HeLa cells. As quantification of intracellular α2-integrin in cells with low accumulation efficiency is unreliable, we focused on cells with efficient α2-integrin accumulation. We set a threshold for cells with high levels of intracellular α2-integrin (defined visually during imaging) and subsequently used the empirical cumulative distribution function to define the respective cell population for every experiment (**Fig. S2**) and the Gaussian Mixture Model to automatically separate cell subpopulations (see **Methods**). Usually, high levels of intracellular α2-integrin were found in 40-50% of HeLa cells transfected with the negative control and these were used for further analysis to yield high quality data.

Screen hits were defined according to individual z-scores of each siRNA normalized to that of the negative controls (see **Methods**). Positive z-scores indicate increased amounts and negative z-scores indicate reduced amounts of intracellular α2-integrin. We considered siRNAs with z-scores of > +/- 1 as primary hits (**Table S2**). In total, 122 genes were assigned as hits in our screen (see **Methods**), of which 115 inhibited and 7 accelerated α2-integrin intracellular accumulation (**Fig. 3A**). Next, we separated the primary hits into strong (z-score > +/- 1.5) and weak effectors (z-score < +/- 1.5). Downregulation of CLTC and DNM2 produced a z-score of -1.5, corresponding to a strong inhibition of α2-integrin traffic on cell arrays (**Fig. 3B**). 26 other genes were classified as strong inhibitors, some outperforming the effect of CLTC and DNM2 downregulation (**Table S2**). For instance, downregulation of syndecan-4, a protein implicated in caveolae-dependent internalization of integrins (Bass et al., 2011), lead to a strong inhibition (z-score = -1.78) of α2-integrin intracellular accumulation. The majority of the inhibitors were characterized as weak effectors (90 out of 115); depletion of CAV1 for 48 h showed reproducible, but weak inhibitory effect (z-score = -1,14). In part, this may reflect the level of protein knockdown achieved during the relatively short incubation period with siRNAs (**Fig. S1**). 7 primary hits of the screen were called “accelerators” (**Table S2**). One of them is ASAP1, a GAP of ARF6 (Randazzo et al., 2007),

previously shown to regulate integrin recycling (Onodera et al., 2012). It was scored as a strong accelerator (z-score = 2.26); that effect caused by the enhanced accumulation of intracellular α2-integrin, likely due to inhibited recycling.

With the exception of kinases and phosphatases which were over-represented (19%) in comparison to the screened library (11%) (**Table S1, Table S2**) no significant representation of protein functional class (assigned based on Gene Ontology terms) was observed among strong effectors. While comparing our primary hits to a genome-wide screen for regulators of transferrin and EGF endocytosis (Collinet et al., 2010), we found that 39 out of 122 of our hits (32%) were reported as regulators of either transferrin or EGF endocytosis and 83 primary hits from our screen appeared to be specific only to α2-integrin intracellular accumulation (**Fig. 3C**).

As endocytic trafficking of integrins is fundamental for regulation of focal adhesion dynamics and cell migration (Morgan et al., 2013, Chao and Kunz, 2009, Caswell and Norman, 2008), we compared the results of our screen to two published relevant RNAi screens (Winograd-Katz et al., 2009, Simpson et al., 2008) (**Fig. 3C**). 161 genes from our experiments were also screened to identify regulators of focal adhesions and cell migration (Winograd-Katz et al., 2009, Simpson et al., 2008). 24 out of 161 genes (15%) were identified as the primary hits for both α2-integrin intracellular accumulation and formation of focal adhesions, for instance, phosphatidylinositol phosphatase PTEN (Mise-Omata et al., 2005). 9 out of 161 genes (5.5 %) were positive in our and cell migration assays.

We observed a fairly large overlap between our primary hits and the components of integrin-primed complexes. Our screen included 45, out of 467 identified non-redundant components of α5β1 and α4β1 integrins (Humphries et al., 2009) and of these, 19 were assigned as potential regulators of α2-integrin intracellular accumulation (e.g., molecular motors KIF2C and cytoplasmic dynein 1 heavy chain 1 DYNC1H1). A recent search for β1-integrin interacting proteins (Böttcher et al., 2012) yielded 96 proteins, from which 11 were tested in our study, and four of these were assigned as primary hits (**Table S2**). For instance, integrin-activating protein Kindlin-1 (Moser et al., 2009), LIMS1, an adaptor protein that connects integrins, small GTPases and EGF signalling pathways (Tu et al., 1999) and RALBP1, a GAP of Rac1 and Cdc42 (Matsubara et al., 1997). Our screen revealed a number of potential novel regulators of α2-integrin trafficking, e.g., KIF18A, a key component of chromosome congression in mitosis (Mayr et al., 2007), induced a strong inhibition of α2-integrin intracellular accumulation when downregulated (**Fig. 3B**).

Validation of potential regulators of α2-integrin intracellular accumulation

For validation the potential regulators of α2-integrin trafficking identified in the siRNA screen described above, we selected 1/5 of the primary hits (23 proteins). One of the selected groups included the kinesins as very little is known about the role of these molecular motors in integrin trafficking, and essentially all kinesins were tested in the primary screen (**Table S1**) (Hirokawa et al., 2009). Validation assays were performed in non-coated multi-well plates under conditions of a direct transfection. Intracellular accumulation was considered as inhibited when the pool of intracellular α2-integrin was reduced by more than 40% compared to the negative control (see **Methods**). We scored potential hits as validated when at least two out of four siRNAs showed the same effect as in the primary screening (**Table S4).** From the 9 primary hit kinesins that are expressed in HeLa cells (**Table S3**), three, namely KIF15, KIF18A and KIF23 were validated as effectors of α2-integrin intracellular accumulation (**Table 1**). As kinesins are important trafficking regulators we extended our investigation beyond the 9 kinesins identified as primary hits in our screen. We re-tested 13 more traffic-related kinesins that were non-hits in the primary screen (**Table S3, S4**) and demonstrated that only KIF13A, a recycling regulator in melanocytes (Delevyoe et al., 2009) affected α2-integrin intracellular accumulation in the validation experiments. As this result was obtained only with the additional siRNAs, but not with the ones used for the primary screen, we did not include KIF13A in the list of the validated hits.

Next, we tested whether decreased levels of intracellular α2-integrin are a direct consequence of inhibited trafficking or reduced protein expression. For this, we measured total amounts of α2-integrin following downregulation of the validated kinesins (**Table 1**). Expression levels of α2-integrin were not affected when KIF15, KIF18A and KIF23 were down-regulated (**Fig. S3**). As these kinesins were shown to play a role in mitosis (Mayr et al., 2007, Tanenbaum et al., 2009, Zhu et al., 2005), we calculated the number of cells remaining after 48h of transfection with the respective siRNAs. Downregulation of KIF23 expression reduced the number of cells by nearly two-fold, whereas downregulation of KIF15 and KIF18A did not induce a significant change (**Table 1**).

To get a better overview about the specificity of our screen we re-tested 14 additional primary hits belonging to diverse functional groups. For this, we chose the molecules that were scored as effectors with multiple siRNAs in the primary screen (**Table S2**). RNAi-mediated inhibition of 7 of these proteins strongly reduced levels of intracellular α2-integrin in the validation assays (**Table 1, Table S4**). Five of these were also classified as strong inhibitors in the primary screen (ARF1, ABL2, ARHGAP6, Myo1A and PTPN11). Suppressed expression of two of these proteins (ARF1 and NF2) did not alter α2-integrin expression levels, suggesting a role for these proteins in α2-integrin trafficking. ITGB1 and Myo1A reduced α2-integrin expression when

downregulated, however these proteins may play a role in α2-integrin trafficking as inhibition of α2-integrin intracellular accumulation was more pronounced than the effects seen on α2-integrin expression (**Table 1**). In contrast, the observed effect on intracellular α2-integrin levels upon ABL2 and ARHGAP6 downregulation was largely due to the reduction in total α2-integrin expression. Down-regulation of only PTPN1 significantly reduced cell numbers (by nearly 35%).

In summary, we could recapitulate the results of the primary screen for 10 out of the 23 hits (43%). For nearly half of them this effect could be attributed to changes of intracellular α2-integrin accumulation, whereas, other primarily act on α2-integrin expression level.

Internalization of α2-integrin is KIF15 dependent

To pull out more detail regarding what appeared to be novel regulators revealed by our targeted screen, we focused on KIF15 as no trafficking-related function has been described for KIF15 so far. RNAi of KIF15 for 48h resulted in a 70% reduction of KIF15 protein levels (**Fig. S4A,C**) and led to a strong inhibition of α2-integrin intracellular accumulation without significant change in α2-integrin expression level and cell numbers (**Table 1, Fig. S3A,B**). Consistent with a decrease in α2-integrin intracellular levels, suppression of KIF15 expression led to a concomitant increase in cell surface α2-integrin (**Fig. S3C**). Moreover, moderate expression of ectopic GFP-tagged KIF15 (Tanenbaum et al., 2009) (3.3-fold as compared to the endogenous protein) (**Fig. S4B,D**) induced an increase in intracellular α2-integrin amounts by approximately 40% (**Fig. 4A,B**), with α2-integrin accumulating at the perinuclear region after 1h of internalization. Over-expression of GFP alone under these conditions had no apparent influence. GFP-tagged KIF15 mostly localized to the cytoplasm (**Fig. 4A**) with occasional localization to the PM, punctate cytoplasmic structures and microtubules. As GFP-tagged murine KIF15 is resistant to human siRNAs we performed rescue experiments, which showed that the siRNA-mediated inhibitory effect of KIF15 on α2-integrin intracellular accumulation was lessened by 30% (**Fig. 4B**) following overexpression of GFP-tagged KIF15. The role of KIF15 in α2-integrin endocytic trafficking was further confirmed by biotin-capture ELISA assays (Margadant et al., 2012, Roberts et al., 2001) (**Fig. 4C**). In addition, endocytosis of β1-integrin was also inhibited as measured by ratiometric quenching antibody-based assay (Arjonen et al., 2012) (**Fig. 4D**). Both assays revealed a lower inhibition rate of integrin trafficking (around 25%) when KIF15 was downregulated as compared to the microscopy-based assay (**Table 1**). This may be attributed to the difference in quantifying the whole cell population in these assays and a defined subpopulation of cells for the microscopy-based assay (see **Methods**). No significant changes in actin and microtubule cytoskeleton were observed

following KIF15 downregulation (**Fig. 4E,F**). Altogether, depletion of KIF15 inhibited α2-integrin intracellular accumulation in different types of cells (**Fig. S3D**).

Next, we analysed at which stage α2-integrin intracellular accumulation is affected when KIF15 is depleted. In cells transfected with the negative control, α2-integrin gradually accumulated within the cells, whereas, downregulation of KIF15 strongly inhibited intracellular accumulation of α2-integrin throughout the assay (5-60 min) (**Fig. 5A,D**). We then tested the effect of KIF15 downregulation on the trafficking of EGF that is degraded in lysosomes (Carpenter and Cohen, 1976) and transferrin that is recycled to the PM (Dickson et al., 1983). In agreement to (Collinet et al., 2010), downregulation of KIF15 had no influence on internalization of both EGF and transferrin cargoes at early time points (**Fig. 5B,C,E,F**). However, later steps of transferrin trafficking were significantly affected by KIF15 downregulation (**Fig. 5E**) with the cargo accumulating in the perinuclear region (**Fig. 5B**). Presumably, the observed effect is due to inhibited recycling of transferrin to the PM. In contrast, EGF endocytic trafficking was not influenced by KIF15 downregulation at any time point (**Fig. 5C,F**).

KIF15 is required for cell surface localization of Dab2

We sought to further investigate the integrin-related trafficking function of KIF15. It was shown that several alternative clathrin adaptors CLASPs are required for integrin internalization (Nishimura and Kaibuchi, 2007, Teckchandani et al., 2009). In contrast, internalization of the transferrin receptor is not dependent upon CLASPs, like Dab2 (Teckchandani et al., 2009, Teckchandani et al., 2012, Maurer and Cooper, 2006, Keyel et al., 2006). In our experiments RNAi of Dab2, ARH and Numb for 48h caused more than 80% reduction of the respective transcripts (**Fig. 6D**) and the condition was used to assess the potential role of these CLASPs in α2-integrin trafficking. The strongest inhibition of α2-integrin endocytosis was obtained by depletion of Dab2 (**Fig. 6A,B,C**). RNAi of ARH had weaker effect, whereas Numb showed no significant inhibition. Our data are in a good agreement with the studies of Chao and Kunz, 2009 and Teckchandani et al., 2012, showing that Dab2 strongly inhibits internalization of β1-integrin when down-regulated. Furthermore, surface levels of integrins β1 and α2 increase in Dab2-deficient Hela cells (Teckchandani et al., 2009).

We next tested whether Dab2 is functionally dependent upon KIF15. In agreement to previous studies (Teckchandani et al., 2009, Chetrit et al., 2011), Dab2 localized to punctate structures that were found both on the PM and intracellularly in HeLa cells imaged in TIRF and epifluorescence modes **(Fig. 7A)**. Downregulation of KIF15 induced more than 40% loss of the cell

surface Dab2 **(Fig. 7C, D)** with a large fraction of Dab2-specific structures being redistributed from the PM to the cytoplasm **(Fig. 7B).** Total level of Dab2 in cells was not changed significantly in these conditions **(Fig. 7B, Fig. S4,F)**. The role of KIF15 in Dab2 distribution was further demonstrated by a 2.7-fold more frequent accumulation of intracellular Dab2 in the perinuclear region following the depletion of KIF15 (**Fig. 7D**), indicating that KIF15 might play a role in recycling pathways. Surprisingly, no significant co-localization between Dab2 and α2-integrin was obtained at 37^{o}C regardless of KIF15 expression levels. It is possible, that trapping of integrin at low temperatures is required as demonstrated for β1-integrin (Teckchandani et al., 2009). Altogether, our data suggest that KIF15 mediates cell surface localization of Dab2 that, in turn, might regulate internalization of α2-integrin.

Discussion

Defective endocytosis of integrins leads to numerous alterations in signalling, cell cycle progression, cell-ECM interactions and the cytoskeleton, crucial processes of cancer initiation, progression and metastasis (Mosesson et al., 2008, Shin et al., 2012, Desgrosellier and Cheresh, 2010). Integrin α2β1 is known as a potent suppressor of breast cancer metastasis (Ramirez et al., 2011), however, little is known about the endocytic trafficking of this heterodimer. We show here that endogenous α2-integrin in HeLa cells passes through a Rab5-specific compartment and ispotentially recycled to the PM via Rab4- and Rab11- specific structures (**Fig. 2**). Interestingly, depletion of not only clathrin, but also caveolin-1 induced a comparably strong inhibition of α2-integrin intracellular accumulation (**Fig. 1F,G**). Both pathways might act in parallel; however, RNAi-based perturbation of individual pathways could invoke broad cellular responses (Doherty and McMahon, 2009). Alternatively, our data opens an intriguing possibility that clathrin- and caveolin-dependent mechanisms might act in a sequential manner. Nevertheless, the endocytic route of unbound α2-integrin differs strongly from the calpain-dependent degradation pathway taken by the antibody-clustered α2-integrin (Rintanen et al., 2012). With the goal to define a significant segment of the universe of proteins affecting α2-integrin cell surface expression, we performed a fluorescent microscopy-based RNAi screen (**Fig. 3**).

In total, 386 genes associated with membrane traffic and cytoskeletal organization, and encompassing most mammalian motor proteins were tested (**Table S1**), with 122 molecules scored as potential regulators of α2-integrin intracellular accumulation (**Fig. 3A, Table S2)**. Predominantly, a reduction in α2-integrin intracellular accumulation was recorded (for 115 potential regulators),

and only 7 molecules increased intracellular accumulation of α2-integrin when downregulated. In the subsequent validation experiments, some of the inhibitors were shown to be reducing the overall expression of α2-integrin in cells, however, specific inhibitors of trafficking, such as KIF15, were also identified. 83 primary hits of our screen might be specific to intracellular accumulation of α2-integrin as they were not identified as regulators of transferrin or EGF endocytosis (**Fig. 3C**, (Collinet et al., 2010)). Possibly, the different outputs of the screens reflect differences between data acquisition (wide field vs confocal microscopy), read-out (monoparametric vs multiparametric), data normalisation procedures, and testing different siRNA libraries. On the other hand, both screens were performed in HeLa cells and unsurprisingly there was a fairly large overlap of our hits (39 out of 122) with the regulators of transferrin and EGF endocytosis (**Fig. 3C**, (Collinet et al., 2010)). Interestingly, nearly half of the interacting partners of β1-integrin (Böttcher et al., 2012), present in our library, were also effectors of α2-integrin trafficking (**Table S2**), but little overlap could be found with the proteomics analysis of interacting partners of the over-expressed and tagged α2-integrin in HT1080 cells (Uematsu et al., 2012). Potentially, this is due to a different cellular context and/or expression levels of integrin. Surprisingly, 24 out of 122 potential regulators of α2-integrin trafficking are known as potential regulators of focal adhesion formation (**Fig. 3C**, (Winograd-Katz et al., 2009)), indicating a functional cross-talk in trafficking of unbound and ligand-bound integrins.

For data validation we chose several subsets of the primary hits. One subset contained 14 functionally heterogeneous molecules that were recorded as hits by multiple siRNAs in the primary screen (**Table S2**) and 7 of them were validated (**Table 1**). Curiously, only two of them NF2 (Merlin) and a small GTPase ARF1 predominantly influenced α2-integrin intracellular accumulation, while others appeared to influence primarily a2-integrin expression levels. ARF1 is a key component of the COPI coatomer complex and one of the most important trafficking regulators (Donaldson and Klausner, 1994, D'Souza-Schorey et al., 2006, Volpicelli-Daley et al., 2005). Potentially, ARF1 inhibits α2-integrin trafficking by regulating recycling to the PM as it was demonstrated for α5-integrin (Krndija et al., 2012), however other functions of ARF1 cannot be excluded. NF2/Merlin may act indirectly by providing a linkage between membrane-associated proteins and the actin cytoskeleton, thus regulating membrane organization (Li et al., 2012, McClatchey and Giovannini, 2005). Conversely, the Drosophila ortholog of NF2/Merlin localizes to the endocytic compartment in S2 cells (McCartney and Fehon, 1996), and it was reported that NF2/Merlin binds to β1-integrin in Schwan cells (Obremski et al., 1998) suggesting a more direct role for these proteins in integrin traffic.

Another subset of potential regulators chosen for validation analysis were kinesins, microtubule-based molecular motors. Systematic analysis of kinesins has already been performed in the context of cell cycle regulation (Tanenbaum et al., 2009, Goshima and Vale, 2003, Neumann et al., 2010, Zhu et al., 2005) and membrane trafficking (Collinet et al., 2010, Paul et al., 2011, Simpson et al., 2012), but information about their roles specifically in integrin trafficking is missing. We observed no effect on α2-integrin trafficking when downregulating 13 kinesins that had no effect in the primary screen (**Table S2**, **Table S4**), indicating high fidelity of our assays. From the 9 kinesins recorded as primary hits, three (KIF15, KIF18A and KIF23) strongly inhibited α2-integrin endocytic trafficking (**Table 1**). As expected, the validation rate of kinesins was lower than that of the regulators targeted with the multiple siRNAs. However, the validated ones are most likely actual trafficking regulators as none of them changed the expression level of α2-integrin. Indeed, KIF15 and KIF23 have been identified as potential regulators of ts-O45-G (temperature sensitive mutant of vesicular stomatitis virus) biosynthetic trafficking (Simpson et al., 2012).

In this study we have focused on KIF15, one of the strongest validated effector of α2-integrin intracellular accumulation. Downregulation of KIF15 inhibited intracellular accumulation of α2- and β1-integrin as shown by several complementing approaches (**Table 1, Fig. 4C,D, Fig. 5A,D**) without having any effect on cell numbers. The latter observation is in agreement with the notion that KIF15 can be displaced by Eg5 (Tanenbaum et al., 2009, Mayer and Forian, 2011) in the organization of bipolar mitotic spindles (Sueishi et al., 2000, Vanneste et al., 2009, Sturgill and Ohi, 2013). In addition, KIF15 was not identified as a regulator of cell cycle progression in a genome-wide RNAi screen (Neumann et al., 2010). KIF15 is expressed in interphase and shows a remarkably different localization in various cells: centrosomes in HeLa cells (Sueishi et al., 2000), actin bundles in fibroblasts and microtubules in terminally post mitotic neurons (Buster et al., 2003). GFP-tagged murine KIF15 localized largely to the cytoplasm in HeLa cells with occasional localization to the PM, microtubules and punctate structures. Similar localization pattern was observed in lung A549 epithelial carcinoma cells and normal human fibroblasts BJ-5ta. Furthermore, downregulation of KIF15 induced inhibition of α2-integrin intracellular accumulation in these cells (**Fig. S3D**), indicating that KIF15 plays a role in integrin trafficking in cancer and normal cells. Altered expression levels of KIF15 did not induce apparent alterations in actin or microtubule cytoskeleton and centrosomes, ruling out the possibility that α2-integrin intracellular accumulation is altered due to general cytoskeletal changes (**Fig. 4,E,F**).

Over-expression of GFP-tagged KIF15, resistant to human siRNAs, partially rescued inhibition of α2-integrin intracellular accumulation caused by KIF15 depletion (**Fig. 4A,B**). In addition, increased cell surface α2-integrin expression was measured following KIF15

downregulation **(Fig. S3C).** These data somewhat contradict the directionality of this motor (Boleti et al., 1996). For instance, downregulation of microtubule plus end-directed motors KIF1C and KIF16B induced reduction of cell surface localization of α5β1 integrin (Theisen et al., 2012) and transferrin recycling (Hoepfner et al., 2005), respectively. Downregulation of KIF15 induced accumulation of transferrin at the perinuclear region (**Fig. 5B**), suggesting that it might function in the trafficking from the perinuclear recycling compartment. On the contrary, internalization of EGF and transferrin was not influenced by the depletion of KIF15 (**Fig. 5B,C,E,F** and (Collinet et al., 2010)).

Altogether, our data indicates the possibility that KIF15 may be involved in the surface delivery of an entry factor required for α2-integrin internalization. Indeed, CLASPs are known to specifically regulate β1-integrin internalization (Nishimura and Kaibuchi, 2007,12, Chao and Kunz, 2009, Ezratty et al., 2005). In agreement with this, we showed that endocytic trafficking of non-clustered α2-integrin might require not only the clathrin-independent, but also clathrin-dependent pathways in HeLa cells (**Fig. 1F,G**). It is known, that downregulation of FXNPXY-signal sorting CLASPs (Keyel et al., 2006), Dab2, ARH, and Numb are required for β1-integrin internalization in a number of migrating cells as well as for disassembly of focal adhesions (Nishimura and Kaibuchi, 2007, Chao and Kunz, 2009). Our RNAi data using microscopy-based α2-integrin endocytosis assay largely confirms these observations with Dab2 being the strongest effector (**Fig. 6**). Similar to endocytosis of LDLR (Keyel et al., 2006, Maurer and Cooper, 2006), downregulation of ARH also inhibited α2-integrin intracellular accumulation by 40% (**Fig. 6B**). In contrast, no effect of ARH depletion on surface expression of β1-integrin was reported (Teckchandani et al., 2009), which may reflect usage of different methodologies. Depletion of Numb, the adaptor with a preference towards α5-integrin (Teckchandani et al., 2009) resulted in no significant change in α2-integrin intracellular accumulation. As Dab2 is known to inhibit internalization of unbound β1-integrin (Teckchandani et al., 2009, Teckchandani et al., 2012) and appeared to be the strongest effector of non-clustered α2-integrin intracellular accumulation, we focused on Dab2 for further analysis. We could show that the downregulation of KIF15 induced re-distribution of punctate Dab2 structures from the PM (**Fig. 7A,C**). Most likely, these are endocytic structures as they were shown to co-localize with clathrin and AP-2 by more than 70% in HeLa, NIH3T3 and ES-2 cells (Chetrit et al., 2011, Teckchandani et al., 2009, Morris and Cooper, 2001). In addition, Dab-2 specific structures were shown to co-localize to unbound β1-integrin by more than 25% (Teckchandani et al., 2009). It is plausible, therefore, that their displacement from the PM inhibits internalization of non-clustered α2-integrin. Dab2 is redistributed from the periphery and accumulates at the perinuclear compartment following

downregulation of KIF15 (**Fig. 7D**), but does not co-localize to transferrin under these conditions. In agreement, ce-Dab-1, *C. elegans* ortholog of Dab2, does not co-localize to Rab11-positive structures (Kamikura and Cooper, 2006). On the other hand, the transferrin distribution might be affected by the mislocalized Dab2, which was shown to regulate recycling of numerous proteins, including transferrin (Fu et al., 2012). As Dab2-mediated internalization of integrins occurs through the clathrin-dependent pathway (Teckchandani et al., 2012, Ezratty et al., 2009, Chao and Kunz, 2009), KIF15 might contribute to the regulation of α2-integrin endocytic fate. Whether KIF15 influences Dab2 distribution through direct binding as demonstrated for the actin-based molecular motor Myosin 6 (Spudich et al., 2007, Morris et al., 2002) or indirectly remains to be answered, particularly, in a frame of cell cycle progression as Dab2 cell surface localization and function in endocytosis is changing throughout the cell cycle (Chetrit et al., 2011). Involvement of KIF15 in clathrin-independent trafficking cannot be ruled out at the present as it was recently demonstrated that kinesins, like KIF13B, enhance cargo recruitment to caveolae (Kanai et al., 2014). Emerging role of KIF15 in trafficking of α2-integrin and possibly other cargoes will be interesting to investigate in a disease context as KIF15 is over-expressed in various tumours (Bidkhori et al., 2013).

Elucidating the molecular mechanisms influencing endocytic trafficking of α2β1 integrin, one of the most important collagen receptor is emerging as an exciting research area. This knowledge is essential for prevention and treatment of diseases associated with integrin-mediated adhesion. Here, we present a microscopy-based assay that is suitable for high-throughput applications and is helpful in systematic identification of novel regulators of α2-integrin intracellular accumulation and/or expression.

Materials and Methods

Cell culture

HeLa cells ATCC (CCL-2) were cultured in MEM (Sigma-Aldrich), A549 cells ATCC (CCL-185) were cultured in F-12K (Sigma-Aldrich), BJ-5ta cells ATCC (CRL-4001) were cultured in 4:1 mixture of DMEM and Medium 199 (Sigma-Aldrich). All media contained 10% FCS, 2 mM glutamine, 100 U/ml penicillin and 100 µg/ml streptomycin. For experiments requiring serum starvation cells were kept in the respective media supplemented with 0.01% (w/v) BSA.

Materials

GFP-Rab5, GFP-Rab7a, mCherry-Rab11b, and mCherry-Rab4a were a gift from Dr. N. Brady (DKFZ/BioQuant, University Heidelberg). GFP-MmKIF15 plasmid and anti-KIF15 antibody were a gift from R. Medema (The Netherlands Cancer Institute). Mouse monoclonal anti-α2-integrin antibody (clone P1E6) was from Merck-Millipore, rabbit monoclonal anti-Dab2 (H-110) and rabbit polyclonal anti-caveolin-1 were from Santa Cruz Biotechnology. Mouse monoclonal anti-Dab2 (clone 52/p96) was from BD Biosciences, mouse monoclonal anti-clathrin and rabbit polyclonal anti-dynamin-2 were from Abcam. Mouse monoclonal anti-α-tubulin (clone DM1A9) was from Cell Signaling, secondary anti-mouse and anti-rabbit antibodies coupled to Alexa-488 and Alexa-647 were from Invitrogen, anti-rabbit antibodies coupled to HRP were from GE Healthcare and anti-mouse antibodies coupled to HRP were from R&D. Transferrin-Alexa568, EGF-Alexa555 and phalloidin-Alexa647 conjugates were from Invitrogen. siRNAs targeting Dab2 (#SI02780316 and #SI02780386), ARH (#SI03042634 and #SI00111657) and Numb (#SI04256994 and #SI03199581) were from Qiagen. All other siRNAs are listed in the **Table S1**.

Transfection of siRNAs and cDNAs

For the reverse transfection on cell arrays 5 µl of 30 µM siRNA was mixed with 3,5 µl Lipofectamine 2000 (Invitrogen) and 3 µl Opti-MEM (Invitrogen) containing 0,4 M sucrose and incubated for 20 min at RT. Thereafter, it was mixed with 7,25 µl of 0,2% gelatine (w/v) in 0,01 % fibronectin (v/v), and transferred to the contact printing with the automated liquid handling robot 'Microlab Star' (Hamilton) on 1-chamber Lab-Tek (Nunc) using eight solid pins PTS 600, which gives the spot size of approx. 400 µm. The spot-to-spot distance was set to 1125 µm, thus a single Lab-Tek fitted 384 spots organized in 12 columns and 32 rows. The whole library of 1084 siRNAs was spotted on 4 Lab-Teks, with 6-12 negative control siRNAs distributed randomly across each layout. $5x10^5$ cells were seeded/ per Lab-Tek. Liquid-phase direct transfection with siRNAs or cDNAs in 8-well µ-slide (Ibidi) was performed using Lipofectamine 2000 according to manufacturer's protocol with $2x10^4$ cells seeded/ per well. Tranfection of cells with siRNA and cDNAs was done 48h and 24h before the assay, respectively.

Western Blotting

1.5 x 10^5 HeLa cells were plated in 12-well plate, tranfected with the respective siRNAs and cDNAs, lysed in 80 ml hot Laemmli buffer, supplied with 100 mM DTT, and separated by 8 % SDS-PAGE. The proteins were transferred to PVDF membrane (Immobilion-P, Merck-Millipore),

unspecific proteins were blocked with 5% milk in PBST, and incubation with the anti-KIF15 and anti-Dab2 antibodies was done at 4°C and RT for 1h, respectively. The proteins of interest were detected by ECL system (GE Healthcare). The luminescence was recorded by Chemiluminescence Detection System (Intas) and quantified by ImageJ (NIH) "Analyze -> Gel" option. Intensity of the relevant band of the blot was expressed as the area of the peak after subtraction of the average background level of the whole blot.

qRT-PCR and RT-PCR

Preparation of total cellular RNA was made using TRIzol reagent (Invitrogen) according to the manufacturer's protocol. cDNA was prepared with MMVL-reverse transcriptase (Ambion) and oligo-dT primer. Power SYBR Green PCR-Mastermix was used for the reaction, which was carried out in StepOnePlus Real-Time PCR system (Applied Biosystems). Relative Dab2, ARH and Numb expression after RNAi was calculated by $2^{\Delta\Delta CT}$ method using expression level of GAPDH as a reference for the quantification. Expression of genes of interest in HeLa cells was tested by RT-PCR with 1-3 sets of primers that were determined by nucleotide BLAST analysis against human genome and trancriptome (http://blast.ncbi.nlm.nih.gov). Primers were either designed using Primer BLAST (http://blast.ncbi.nlm.nih.gov/tools/primer-blast/) or used as published (Jaulin et al., 2007).

Fluorescence microscopy based α2-integrin measurements

Cells were serum-starved for 14h, overlaid with the 10 µg/ml anti-α2-integrin antibody in MEM-BSA for 1h on ice, then shortly washed twice with ice-cold MEM-BSA to remove the excess of the antibody, and incubated with pre-warmed MEM-BSA at 37°C to internalize non-clustered α2-integrin. After the internalization cells were rinsed with PBS, surface bound antibody was removed with acetic buffer (0,5% (v/v) acetic acid, 0,5M NaCl, pH 2,6) for 30-40 s, and fixed with 2% PFA for 20 min at RT. Cells were permeabilized with 0,2% (w/v) saponin in 10% (v/v) FCS in PBS and incubated with the secondary antibodies for 1h at RT. When measuring total α2-integrin levels, the treatment with the acetic buffer was omitted, cells permeabilized with 0,2% (w/v) saponin in 10% (v/v) FCS in PBS and stained with the primary and secondary antibodies. α2-integrin on cell surface were measured by fixing cells with 2% PFA for 20 min at RT, quenching with 30 mM glycin for 5 min at RT and staining with the primary and secondary antibodies. Clustering by antibody was induced as described in (Upla et al., 2004) by sequential incubation of cells with the primary anti-α2-integrin and then with secondary antibodies on ice for 1h each. Then cells were shortly washed twice with ice-cold MEM-BSA and incubated with the pre-warmed MEM-BSA at 37°C to

internalize antibody-clustered α2-integrin. Nuclei were stained with 0,1 µg/ml Hoechst 33342 dye. In order to estimate the efficiency of acid stripping, we compared the average vales of total α2-integrin specific fluorescence, surface localized α2-integrin and intracellular non-clustered α2-integrin following 60 min of internalization using the same parameters for imaging and image analysis. The highest average fluorescence intensity was obtained for total α2-integrin (100%), the levels of non-clustered intracellular α2-integrin obtained after acid stripping were 19.2% and surface α2-integrin specific fluorescence were 69,5%, making up to 88,7% of the total α2-integrin fluorescence.

Surface biotinylation based α2-integrin internalization assay

The internalization of biotinylated α2-integrin was measured as described in Roberts et al., 2001 and amount of biotinylated α2-integrin was determined by capture-ELISA.

Quenching antibody-based β1-integrin internalization assay

The assay was essentially performed as described in Arjonen et al., 2012 using CD29 clone K20 antibodies (Beckman, Coultier) conjugated to AlexaFluor 488 for β1-integrin labelling. After cell fixation, fluorescence intensities were measured by EnVision Multilabel Plate Reader (Perkin Elmer).

EGF and transferrin internalization assays

Cells were serum-starved for 14 h before the assay; then EGF-Alexa555 was added to MEM-BSA medium to a final concentration of 100 ng/ml and cells were incubated at 37°C for different time points. Surface attached EGF-Alexa555 was removed with acidic buffer (50 mM glycine, 150 mM NaCl, pH 3.0). For transferrin endocytic trafficking assay cells were serum-starved for 1h, then tranferrin-Alexa568 was added to MEM-BSA medium to a final concentration of 25 µg/ml. Cells were fixed with 3% PFA for 20 min at RT.

Image acquisition by wide-field, confocal and TIRF microscopy

Image acquisition in wide-field mode was done on Olympus IX81 Scan^R automated inverted microscope (Olympus Biosystems) controlled by Scan^R acquisition software. 10x/0.4 NA air

objective (UPlanSApo; Olympus Biosystems) was used for the primary screening on cell arrays and 20x/0.75 NA air objective (UPlanSApo; Olympus Biosystems) was used for all other experiments. Excitation wavelength = 450-490 nm and emission wavelength = 500 – 550 nm was used to image α2-integrin, excitation wavelength = 426-446 nm, emission wavelength = 460-500 nm - to image EGF-Alexa555, and 545-580 nm excitation and 610-700 emission wavelength - to image transferrin-Alexa568. Excitation wavelength = 325-375 nm, emission wavelength = 435-475 nm was used to image nuclei in all assays. Confocal imaging was performed a confocal laser scanning microscope TCS SP5 (Leica Microsystems) using a 63x oil immersion objective (HCX PL APO 63x/1.4-0.6 Oil CS) and 94 µm diameter pinhole. 488, 561 and 633 nm laser lines were used for the excitation of GFP or Alexa488, mCherry or Alexa568, and Alexa 647, respectively. TIRF was performed on Nikon Eclipse Ti TIRF microscope with Nikon Apo TIFR 60x NA 1.49 objective. 488 and 640 nm laser lines were used for excitation of Alexa488 and Alexa647, respectively.

Co-localization analysis

Co-localization of internalized α2-integrin with overexpressed Rabs in the multi-channelled single confocal plane was done in Image J. The image background was subtracted using a rolling ball algorithm, noise was removed by Gaussian Blur filter and individual structures of more than 10 pixels size were binarized and overlapped. In total, peripheral regions of more than 5 cells/ Rab were used for the analysis with more than 120 structures analysed per cell.

Statistical data analysis

During the primary screening, one image completely encompassed an individual spot. Prior to quantification of the internalized integrin-specific fluorescence intensity, background signal was subtracted applying a rolling ball algorithm (Scan^R Analysis module (Olympus)). All images were subject to visual control. The nuclei of individual cells were identified by intensity module and the regions of nuclei were expanded so as to encompass a maximum area of cell without touching the neighboring ones. Cell densities were optimized to reach 70-90% confluence to secure clear cell-to-cell separation. As the majority of intracellular α2-integrin specific fluorescence was clustered in the region of interest, the method allowed unbiased data quantification. For the statistical analysis of the primary screening data R package (http://cran.r-project.org/) and cellHTS from Bioconductor (http://www.bioconductor.org/) were used. At first, 2% of the cells with the highest integrin-specific fluorescence intensities were excluded for each imaged spot, remaining cell intensities were averaged, and B-score normalization (Brideau et al., 2003) was applied to calculate a correction

factor for each spot, which would account for spatial effects and between-plate artifacts.

To reliably quantify α2-integrin intracellular accumulation, we removed cells with weak endocytic trafficking using threshold, which was set for every experiment separately, according the negative controls and kept the same for all samples within the experiment. Gaussian Mixture Model (Bowman and Azzalini, 1997) was used to automatically cluster the cells into two subpopulations (with high and low efficiencies of α2-integrin intracellular accumulation) assuming that in each subpopulation cells are normally distributed. The median intracellular α2-integrin signal intensities and cell numbers of each subpopulation was calculated for every spot. Then, the median signal intensity of cells with efficient accumulation was multiplied to the number of such cells and divided by the total cell numbers in every spot. This ratio was normalized against the median of the negative controls on each cell array. Eventually, median z-score of 5-8 individual replicates of every siRNA was calculated and one-sided, one-sample Welch's t-test was used to compute significance values. A gene was considered as a primary hit when either one out of two tested siRNAs, at least two siRNAs out of six tested, or at least three siRNAs out of more than eight siRNAs tested had a consistent inhibitory or acceleratory effect on α2-integrin intracellular accumulation. More than 3000 cells were analysed for every siRNA in the primary screen.

For the validation experiments in 8-chamber µ-slides 30 to 42 images/ well were taken and analyzed. All other steps of the analysis were the same as in the primary screening, except that a threshold, separating cells with high and low endocytosis, was set manually. For transferrin and EGF trafficking assays all cells in population were taken for the analysis. Statistical significance of difference between experiments throughout this study was tested by Student's two-tailed t-test for samples with uneven variance.

Acknowledgements

We thank Prof. R. H. Medema (Netherlands Cancer Institute) for the antibodies labelling KIF15 and cDNA encoding KIF15. We thank Prof R. Fässler (MPI Martinsried, Germany) and Dr H. Hamidi (Centre of Biotechnology, University Turku, Finland) for thorough reading of the manuscript and comments. This work was supported by BMBF FORSYS ViroQuant (#0313923), EU FP7 “MEHTRICS” (HEALTH-F5-2011-278758) and Excellence Cluster CellNetworks (EXC81), Heidelberg University. A.E. is supported by LGFG fellowship of Graduate Academy of Heidelberg University.

References

Arjonen, A., Alanko, J., Veltel, S. and Ivaska, J. (2012). Distinct recycling of active and inactive β1 integrins. *Traffic* **13**, 610–25.

Bass, M. D., Williamson, R. C., Nunan, R. D., Humphries, J. D., Byron, A., Morgan, M. R., Martin, P. and Humphries, M. J. (2011). A Syndecan-4 Hair Trigger Initiates Wound Healing through Caveolin- and RhoG-Regulated Integrin A2-integrinEndocytosis. *Dev. cell* **21**, 681–93.

Bergelson, J. M., Shepley, M. P., Chan, B. M., Hemler, M. E. and Finberg, R. W. (1992). Identification of the integrin α2-integrinVLA-2 as a receptor for echovirus 1. *Science* **255**, 1718–20.

Bidkhori, G., Narimani, Z., Hosseini Ashtiani, S., Moeini, A., Nowzari-Dalini, A., Masoudi-Nejad, A. (2013) Reconstruction of an integrated genome-scale co-expression network reveals key modules involved in lung adenocarcinoma. *Plos One* **Jul 11**, 67552.

Boleti, H., Karsenti, E. and Vernos, I. (1996). Xklp2, a Novel Xenopus Centrosomal Kinesin-like Protein Required for Centrosome Separation during Mitosis. *Cell* **84**, 49–59.

Böttcher, R. T., Stremmel, C., Meves, A., Meyer, H., Widmaier, M., Tseng, H.-Y. and Fässler, R. (2012). Sorting nexin 17 prevents lysosomal degradation of β1 integrins by binding to the β1-integrin α2-integrintail. *Nat. Cell Biol.* **14**, 584–92.

Bowman, A. W. and Azzalini, A. (1997). *Applied smoothing techniques for data analysis*. Oxford: Clarendon Press.

Brideau, C., Gunter, B., Pikounis, B. and Liaw, A. (2003). Improved statistical methods for hit selection in high-throughput screening. *J Biomol Screen* **8**, 634–47.

Buster, D. W., Baird, D. H., Yu, W., Solowska, J. M., Chauvière, M., Mazurek, A., Kress, M. and Baas, P. W. (2003). Expression of the mitotic kinesin Kif15 in postmitotic neurons: implications for neuronal migration and development. *J. Neurocytol.* **32**, 79–96.

Carpenter, G. and Cohen, S. (1976). 125I-labeled human epidermal growth factor. Binding, internalization, and degradation in human fibroblasts. *J. Cell Biol.* **71**, 159–71.

Caswell, P. T. and Norman, J. C. (2006). Integrin A2-integrintrafficking and the control of cell migration. *Traffic* **7**, 14–21.

Caswell, P. and Norman, J. (2008). Endocytic transport of integrins during cell migration and invasion. *Trends Cell Biol.* **18**, 257–63.

683 **Caswell, P. T., Spence, H. J., Parsons, M., White, D. P., Clark, K., Cheng, K. W., Mills, G. B.,**
684 **Humphries, M. J., Messent, A. J., Anderson, K. I., et al.** (2007). Rab25 associates with
685 alpha5beta1 integrin α2-integrinto promote invasive migration in 3D microenvironments. *Dev.*
686 *cell* **13**, 496–510.

687 **Caswell, P. T., Vadrevu, S. and Norman, J.** (2009). Integrins: masters and slaves of endocytic
688 transport. *Nat. Rev. Mol. Cell Biol.* **10**, 843–53.

689 **Chao, W.-T. and Kunz, J.** (2009). Focal adhesion disassembly requires clathrin-dependent
690 endocytosis of integrins. *FEBS Lett.* **583**, 1337–1343.

691 **Chen, J., Diacovo, T. G., Grenache, D. G., Santoro, S. A. and Zutter, M. M.** (2002). The alpha(2)
692 integrin α2-integrinsubunit-deficient mouse: a multifaceted phenotype including defects of
693 branching morphogenesis and hemostasis. *Am. J. Pathol.* **161**, 337–44.

694 **Chetrit, D., Barzilay, L., Horn, G., Bielik, T., Smorodinsky, N. I. and Ehrlich, M.** (2011).
695 Negative regulation of the endocytic adaptor disabled-2 (Dab2) in mitosis. *J. Biol. Chem.* **286**,
696 5392–403.

697 **Collinet, C., Stoter, M., Bradshaw, C. R., Samusik, N., Rink, J. C., Kenski, D., Habermann, B.,**
698 **Buchholz, F., Henschel, R., Mueller, M. S., et al.** (2010). Systems survey of endocytosis by
699 multiparametric image analysis. *Nature* **464**, 243–249.

700 **D'Souza-Schorey, C. and Chavrier, P.** (2006). ARF proteins: roles in membrane traffic and
701 beyond. *Nat. Rev. Mol. Cell Biol.* **7**, 347–358.

702 **Day, P., Riggs, K. A., Hasan, N., Corbin, D., Humphrey, D. and Hu, C.** (2011). Syntaxins 3 and
703 4 mediate vesicular trafficking of ⟨5β1 and ⟨3β1 integrins and cancer cell migration. *Int. J.*
704 *Oncol.* **39**, 863–71.

705 **De Fougerolles, A. R., Sprague, A. G., Nickerson-Nutter, C. L., Chi-Rosso, G., Rennert, P. D.,**
706 **Gardner, H., Gotwals, P. J., Lobb, R. R. and Koteliansky, V. E.** (2000). Regulation of
707 inflammation by collagen-binding integrins alpha1beta1 and alpha2beta1 in models of
708 hypersensitivity and arthritis. *J. Clin. Invest.* **105**, 721–9.

709 **Delevoye, C., Hurbain, I., Tenza, D., Sibarita, J.-B., Uzan-Gafsou, S., Ohno, H., Geerts, W. J.**
710 **C., Verkleij, A. J., Salamero, J., Marks, M. S., et al.** (2009). AP-1 and KIF13A coordinate
711 endosomal sorting and positioning during melanosome biogenesis. *J. Cell Biol.* **187**, 247–64.

712 **Desgrosellier, J. S. and Cheresh, D. A.** (2010). Integrins in cancer: biological implications and
713 therapeutic opportunities. *Nat. Rev. Cancer* **10**, 9–22.

Dickson, R. B., Hanover, J. A., Willingham, M. C. and Pastan, I. (1983). Prelysosomal divergence of transferrin and epidermal growth factor during receptor-mediated endocytosis. *Biochemistry* **22**, 5667–74.

Doherty, G. J. and McMahon, H. T. (2009). Mechanisms of endocytosis. *Annu. Rev. Biochem.* **78**, 857–902.

Donaldson, J. G. and Klausner, R. D. (1994). ARF: a key regulatory switch in membrane traffic and organelle structure. *Curr. Opin. Cell Biol.* **6**, 527–32.

Dozynkiewicz MA, Jamieson NB, Macpherson I, Grindlay J, van den Berghe PV, von Thun A, Morton JP, Gourley C, Timpson P, Nixon C, McKay CJ, Carter R, Strachan D, Anderson K, Sansom OJ, Caswell PT, Norman JC. (2012) Rab25 and CLIC3 collaborate to promote integrin α2-integrinrecycling from late endosomes/lysosomes and drive cancer progression**.** *Dev Cell*, **22**, 131-45.

Eble, J. A. (2005). Collagen-Binding Integrins as Pharmaceutical Targets. *Curr. Pharm. Des.* **11**, 867–880.

Eckes, B., Zigrino, P., Kessler, D., Holtkötter, O., Shephard, P., Mauch, C. and Krieg, T. (2000). Fibroblast-matrix interactions in wound healing and fibrosis. *Matrix Biol.* **19**, 325–32.

Emsley, J., Knight, C. G., Farndale, R. W., Barnes, M. J. and Liddington, R. C. (2000). Structural basis of collagen recognition by integrin α2-integrinalpha2beta1. *Cell* **101**, 47–56.

Erfle, H., Neumann, B., Liebel, U., Rogers, P., Held, M., Walter, T., Ellenberg, J. and Pepperkok, R. (2007). Reverse transfection on cell arrays for high content screening microscopy. *Nat Protoc* **2**, 392–399.

Erfle, H., Eskova, A., Reymann, J. and Starkuviene, V. (2011). Cell arrays and high-content screening. *Methods Mol. Biol.* **785**, 277–87.

Ezratty, E. J., Partridge, M. A. and Gundersen, G. G. (2005). Microtubule-induced focal adhesion disassembly is mediated by dynamin and focal adhesion kinase. *Nat. Cell Biol.* **7**, 581–90.

Ezratty, E. J., Bertaux, C., Marcantonio, E. E. and Gundersen, G. G. (2009). Clathrin mediates integrin α2-integrinendocytosis for focal adhesion disassembly in migrating cells. *J. Cell Biol.* **187**, 733–47.

Feire, A. L., Koss, H. and Compton, T. (2004). Cellular integrins function as entry receptors for human cytomegalovirus via a highly conserved disintegrin-like domain. *Proc. Natl. Acad. Sci.*

U.S.A. **101**, 15470–5.

Fleming, F. E., Graham, K. L., Takada, Y. and Coulson, B. S. (2010). Determinants of the specificity of rotavirus interactions with the {alpha}2{beta}1 integrin. *J. Biol. Chem.* **286**, 6165–74.

Fu, L., Rab, A., Tang, L. P., Rowe, S. M., Bebok, Z. and Collawn, J. F. (2012). Dab2 is a key regulator of endocytosis and post-endocytic trafficking of the cystic fibrosis transmembrane conductance regulator. *Biochem. J.***441**, 633–43.

Goshima, G. and Vale, R. D. (2003). The roles of microtubule-based motor proteins in mitosis: comprehensive RNAi analysis in the Drosophila S2 cell line. *J. Cell Biol.* **162**, 1003–16.

Hansen, C. G. and Nichols, B. J. (2009). Molecular mechanisms of clathrin-independent endocytosis. *J. Cell. Sci.* **122**, 1713–21.

Heino, J., Ignotz, R. A., Hemler, M. E., Crouse, C. and Massague, J. (1989). Regulation of cell adhesion receptors by transforming growth factor- beta. Concomitant regulation of integrins that share a common beta 1 subunit. *J. Biol. Chem.* **264**, 380–388.

Hemler, M. E., Elices, M. J., Chan, B. M., Zetter, B., Matsuura, N. and Takada, Y. (1990). Multiple ligand binding functions for VLA-2 (alpha 2 beta 1) and VLA-3 (alpha 3 beta 1) in the integrin α2-integrinfamily. *Cell Differ. Dev.* **32**, 229–38.

Hirokawa, N., Noda, Y., Tanaka, Y. and Niwa, S. (2009). Kinesin superfamily motor proteins and intracellular transport. *Nat. Rev. Mol. Cell Biol.* **10**, 682–696.

Hoepfner, S., Severin, F., Cabezas, A., Habermann, B., Runge, A., Gillooly, D., Stenmark, H. and Zerial, M. (2005) Modulation of Receptor Recycling and Degradation by the Endosomal Kinesin KIF16B. *Cell* **121**, 437-450.

Huang, C., Lu, C. and Springer, T. A. (1997). Folding of the conserved domain but not of flanking regions in the integrin α2-integrinbeta2 subunit requires association with the alpha subunit. *Proc. Natl. Acad. Sci. U.S.A.* **94**, 3156–61.

Humphries, J. D., Byron, A. and Humphries, M. J. (2006). Integrin A2-integrinligands at a glance. *J. Cell. Sci.* **119**, 3901–3.

Humphries, J. D., Byron, A., Bass, M. D., Craig, S. E., Pinney, J. W., Knight, D. and Humphries, M. J. (2009). Proteomic analysis of integrin-associated complexes identifies RCC2 as a dual regulator of Rac1 and Arf6. *Sci Signal* **2**, ra51.

Hynes, R. O. (1992). Integrins: versatility, modulation, and signaling in cell adhesion. *Cell* **69**, 11–25.

Hynes, R. O. (2002). Integrins: Bidirectional, Allosteric Signaling Machines. *Cell* **110**, 673–687.

Jaulin, F., Xue, X., Rodriguez-Boulan, E. and Kreitzer, G. (2007). Polarization-dependent selective transport to the apical membrane by KIF5B in MDCK cells. *Dev. cell* **13**, 511–22.

Kamikura, D. and Cooper, J. (2006). Clathrin Interaction and Subcellular Localization of Ce- DAB- 1, an Adaptor for Protein Secretion in Caenorhabditis elegans. *Traffic* **7**, 324–336.

Kanai, Y., Wang, D., Hirokawa, N. (2014). KIF13B enhances the endocytosis of LRP1 by recruiting LRP1 to caveolae. *J Cell Biol*. **204**, 395-408.

Karjalainen, M., Kakkonen, E., Upla, P., Paloranta, H., Kankaanpää, P., Liberali, P., Renkema, G. H., Hyypiä, T., Heino, J. and Marjomäki, V. (2008). A Raft-derived, Pak1-regulated entry participates in alpha2beta1 integrin-dependent sorting to caveosomes. *Mol. Biol. Cell* **19**, 2857–69.

Keyel, P. A., Mishra, S. K., Roth, R., Heuser, J. E., Watkins, S. C. and Traub, L. M. (2006). A single common portal for clathrin-mediated endocytosis of distinct cargo governed by cargo-selective adaptors. *Mol. Biol. Cell* **17**, 4300–17.

Kramer, R. H. and Marks, N. (1989). Identification of integrin α2-integrincollagen receptors on human melanoma cells. *J. Biol. Chem.* **264**, 4684–8.

Krndija, D., Münzberg, C., Maass, U., Hafner, M., Adler, G., Kestler, H. A., Seufferlein, T., Oswald, F. and Von Wichert, G. (2012). The phosphatase of regenerating liver 3 (PRL-3) promotes cell migration through Arf-activity-dependent stimulation of integrin α2-integrin⟨5 recycling. *J. Cell. Sci.* **125**, 3883–92.

Li, W., Cooper, J., Karajannis, M. A. and Giancotti, F. G. (2012). Merlin: a tumour suppressor with functions at the cell cortex and in the nucleus. *EMBO rep*. **13**, 204–15.

Lobert, V.H., Brech. A., Pedersen, N.M., Wesche, J., Oppelt, A., Malerød, L., Stenmark, H. (2010). Ubiquitination of alpha 5 beta 1 integrin α2-integrincontrols fibroblast migration through lysosomal degradation of fibronectin-integrin α2-integrincomplexes. *Dev Cell* **19,** 148-59**.**

Londrigan, S. L., Graham, K. L., Takada, Y., Halasz, P. and Coulson, B. S. (2003). Monkey rotavirus binding to alpha2beta1 integrin α2-integrinrequires the alpha2 I domain and is facilitated by the homologous beta1 subunit. *J. Virol.* **77**, 9486–501.

Mai, A., Veltel, S., Pellinen, T., Padzik, A., Coffey, E., Marjomäki, V. and Ivaska, J. (2011). Competitive binding of Rab21 and p120RasGAP to integrins regulates receptor traffic and migration. *J. Cell Biol.* **194**, 291–306.

Margadant, C., Kreft, M., de Groot, D-J., Norman, J.C. and Sonnenberg A. (2012). Distinct Roles of Talin and Kindlin in Regulating Integrin A2-integrina5b1 Function and Trafficking. *Curr. Biol*. **22**, 1554-1563.

Margadant, C., Monsuur, H. N., Norman, J. C. and Sonnenberg, A. (2011). Mechanisms of integrin α2-integrinactivation and trafficking. *Curr. Opin. Cell Biol.* **23**, 607–614.

Matsubara, K., Hinoi, T., Koyama, S. and Kikuchi, A. (1997). The post-translational modifications of Ral and Rac1 are important for the action of Ral-binding protein 1, a putative effector protein of Ral. *FEBS Lett.* **410**, 169–74.

Maurer, M. E. and Cooper, J. A. (2006). The adaptor protein Dab2 sorts LDL receptors into coated pits independently of AP-2 and ARH. *J. Cell. Sci.* **119**, 4235–46.

Mayer, T. U. and Florian, S. (2011). Modulated microtubule dynamics enable Hklp2/Kif15 to assemble bipolar spindles. *Cell Cycle* **10**, 3533–44.

Mayr, M. I., Hümmer, S., Bormann, J., Grüner, T., Adio, S., Woehlke, G. and Mayer, T. U. (2007). The human kinesin Kif18A is a motile microtubule depolymerase essential for chromosome congression. *Curr. Biol.* **17**, 488–98.

McCartney, B. M. and Fehon, R. G. (1996). Distinct cellular and subcellular patterns of expression imply distinct functions for the Drosophila homologues of moesin and the neurofibromatosis 2 tumor suppressor, merlin. *J. Cell Biol.* **133**, 843–52.

McClatchey, A. I. and Giovannini, M. (2005). Membrane organization and tumorigenesis--the NF2 tumor suppressor, Merlin. *Genes Dev.* **19**, 2265–77.

Mise-Omata, S., Obata, Y., Iwase, S., Mise, N. and Doi, T. S. (2005). Transient strong reduction of PTEN expression by specific RNAi induces loss of adhesion of the cells. *Biochem. Biophys. Res. Commun.* **328**, 1034–42.

Morgan, MR, Hamidi, H., Bass, MD., Warwood, S., Ballestrem, C., and Humphries MJ. (2013). Syndecan-4 phosphorylation is a control point of integrin recycling. *Cell Dev* **24**, 472–485.

Morris, SM., Arden, SD., Roberts, RC., Kendrick-Jones, J., Cooper, JA., Luzio, JP., Buss, F.

(2002). Myosin VI binds to and localises with Dab2, potentially linking receptor-mediated endocytosis and the actin cytoskeleton. *Traffic*, **3**, 331-41.

Morris, S.M., and Cooper J. (2001). Disabled-2 Colocalizes with the LDLR in Clathrin-Coated Pits and Interacts with AP-2. *Traffic* **2**, 111-123.

Moser, M., Legate, K. R., Zent, R. and Fässler, R. (2009). The tail of integrins, talin, and kindlins. *Science* **324**, 895–9.

Mosesson, Y., Mills, G. B. and Yarden, Y. (2008). Derailed endocytosis: an emerging feature of cancer. *Nat. Rev. Cancer* **8**, 835–50.

Neumann, B., Walter, T., Heriche, J.-K., Bulkescher, J., Erfle, H., Conrad, C., Rogers, P., Poser, I., Held, M., Liebel, U., et al. (2010). Phenotypic profiling of the human genome by time-lapse microscopy reveals cell division genes. *Nature* **464**, 721–727.

Ning, Y., Buranda, T. and Hudson, L. (2007) Activated Epidermial Growth Factor Receptor Induces Integrin A2-integrina2 Internalization via Caveolea/Raft-dependent Endocytic Pathway. *J Biol Chem* 282, 6380-7.

Nishimura, T. and Kaibuchi, K. (2007). Numb controls integrin α2-integrinendocytosis for directional cell migration with aPKC and PAR-3. *Dev. cell* **13**, 15–28.

Obremski, V. J., Hall, A. M. and Fernandez-Valle, C. (1998). Merlin, the neurofibromatosis type 2 gene product, and beta1 integrin α2-integrinassociate in isolated and differentiating Schwann cells. *J. Neurobiol.* **37**, 487–501.

Onodera, Y., Nam, J.-M., Hashimoto, A., Norman, J. C., Shirato, H., Hashimoto, S. and Sabe, H. (2012). Rab5c promotes AMAP1-PRKD2 complex formation to enhance β1 integrin α2-integrinrecycling in EGF-induced cancer invasion. *J. Cell Biol.* **197**, 983–96.

Paul, P., Van den Hoorn, T., Jongsma, M. L. M., Bakker, M. J., Hengeveld, R., Janssen, L., Cresswell, P., Egan, D. A., Van Ham, M., Ten Brinke, A., et al. (2011). A Genome-wide multidimensional RNAi screen reveals pathways controlling MHC class II antigen presentation. *Cell* **145**, 268–83.

Pellinen, T., Arjonen, A., Vuoriluoto, K., Kallio, K., Fransen, J. A. M. and Ivaska, J. (2006). Small GTPase Rab21 regulates cell adhesion and controls endosomal traffic of {beta}1-integrins. *J. Cell Biol.* **173**, 767–780.

Powelka, A. M., Sun, J., Li, J., Gao, M., Shaw, L. M., Sonnenberg, A. and Hsu, V. W. (2004).

Stimulation-Dependent Recycling of Integrin A2-integrinβ1 Regulated by ARF6 and Rab11. *Traffic* **5**, 20–36.

Ramirez, N. E., Zhang, Z., Madamanchi, A., Boyd, K. L., O'Rear, L. D., Nashabi, A., Li, Z., Dupont, W. D., Zijlstra, A. and Zutter, M. M. (2011). The ⟨2β1 integrin α2-integrinis a metastasis suppressor in mouse models and human cancer. *J. Clin. Invest.* **121**, 226–37.

Randazzo, P. A., Inoue, H. and Bharti, S. (2007). Arf GAPs as regulators of the actin cytoskeleton. *Biol. Cell* **99**, 583–600.

Rintanen, N., Karjalainen, M., Alanko, J., Paavolainen, L., Mäki, A., Nissinen, L., Lehkonen, M., Kallio, K., Cheng, R. H., Upla, P., et al. (2012). Calpains promote ⟨2β1 integrin α2-integrinturnover in nonrecycling integrin α2-integrinpathway. *Mol. Biol. Cell* **23**, 448–63.

Roberts, M., Barry, S., Woods, A., Van der Sluijs, P., Norman, J (2001). PDGF-regulated rab4-dependent recycling of alphavbeta3 integrin α2-integrinfrom early endosomes is necessary for cell adhesion and spreading. *Curr. Biol.* **11**, 1392–402.

Santoro, S. A. (1999). Platelet surface collagen receptor polymorphisms: variable receptor expression and thrombotic/hemorrhagic risk. *Blood* **93**, 3575–7.

Shi, F. and Sottile, J. (2008). Caveolin-1-dependent beta1 integrin α2-integrinendocytosis is a critical regulator of fibronectin turnover. *J. Cell. Sci.* **121**, 2360–71.

Shin, S., Wolgamott, L. and Yoon, S.-O. (2012). Integrin A2-integrintrafficking and tumor progression. *Int J Cell Biol* **2012**, 516789.

Simpson, K. J., Selfors, L. M., Bui, J., Reynolds, A., Leake, D., Khvorova, A. and Brugge, J. S. (2008). Identification of genes that regulate epithelial cell migration using an siRNA screening approach. *Nat. Cell Biol.* **10**, 1027–38.

Simpson, J. C., Joggerst, B., Laketa, V., Verissimo, F., Cetin, C., Erfle, H., Bexiga, M. G., Singan, V. R., Hériché, J.-K., Neumann, B., et al. (2012). Genome-wide RNAi screening identifies human proteins with a regulatory function in the early secretory pathway. *Nat. Cell Biol.* **14**, 764–74.

Skalski, M., Yi, Q., Kean, M. J., Myers, D. W., Williams, K. C., Burtnik, A. and Coppolino, M. G. (2010). Lamellipodium extension and membrane ruffling require different SNARE-mediated trafficking pathways. *BMC Cell Biol.* **11**, 62.

Spudich, G., Chibalina, MV., Au, JS., Arden, SD., Buss, F., Kendrick-Jones, J. (2007). Myosin

VI targeting to clathrin-coated structures and dimerization is mediated by binding to Disabled-2 and PtdIns(4,5)P2. *Nat Cell Biol*. **9**, 176-83.

Sturgill, EG., Ohi, R. (2012) Kinesin-12 differentially affects spindle assembly depending on its microtubule substrate**.** *Curr Biol*, **22**, 1280-90.

Sueishi, M., Takagi, M. and Yoneda, Y. (2000). The forkhead-associated domain of Ki-67 antigen interacts with the novel kinesin-like protein Hklp2. *J. Biol. Chem.* **275**, 28888–92.

Takada, Y., Ye, X. and Simon, S. (2007). The integrins. *Genome Biol.* **8**, 215.

Tanenbaum, M. E., Macůrek, L., Janssen, A., Geers, E. F., Alvarez-Fernández, M. and Medema, R. H. (2009). Kif15 cooperates with eg5 to promote bipolar spindle assembly. *Curr. Biol.* **19**, 1703–11.

Teckchandani, A., Toida, N., Goodchild, J., Henderson, C., Watts, J., Wollscheid, B. and Cooper, J. A. (2009). Quantitative proteomics identifies a Dab2/integrin α2-integrinmodule regulating cell migration. *J. Cell Biol.* **186**, 99–111.

Teckchandani, A., Mulkearns, E. E., Randolph, T. W., Toida, N. and Cooper, J. A. (2012). The clathrin adaptor Dab2 recruits EH domain scaffold proteins to regulate integrin α2-integrinβ1 endocytosis. *Mol. Biol. Cell* **23**, 2905–16.

Theisen, U., Straube, E. and Straube, A. (2012). Directional Persistence of Migrating Cells Requires Kif1C-Mediated Stabilization of Trailing Adhesions. *Dev. Cell* **23**, 1153–1166.

Tiwari, S., Askari, J. A., Humphries, M. J. and Bulleid, N. J. (2011a). Divalent cations regulate the folding and activation status of integrins during their intracellular trafficking. *J. Cell. Sci.* **124**, 1672–80.

Tiwari, A., Jung, J.-J., Inamdar, S. M., Brown, C. O., Goel, A. and Choudhury, A. (2011b). Endothelial cell migration on fibronectin is regulated by syntaxin 6-mediated alpha5beta1 integrin α2-integrinrecycling. *J. Biol. Chem.* **286**, 36749–61.

Tu, Y., Li, F., Goicoechea, S. and Wu, C. (1999). The LIM-Only Protein PINCH Directly Interacts with Integrin-Linked Kinase and Is Recruited to Integrin-Rich Sites in Spreading Cells. *Mol. Cell. Biol.* **19**, 2425–2434.

Uematsu, T., Konishi, C., Hoshino, D., Han, X., Tomari, T., Egawa, N., Takada, Y., Isobe, T., Seiki, M. and Koshikawa, N. (2012). Identification of proteins that associate with integrin α2-

integrin⟨2 by proteomic analysis in human fibrosarcoma HT-1080 cells. *J. Cell. Physiol.* **227**, 3072–9.

Upla, P., Marjomaki, V., Kankaanpaa, P., Ivaska, J., Hyypia, T., Van der Goot, F. G. and Heino, J. (2004). Clustering Induces a Lateral Redistribution of {alpha}2{beta}1 Integrin A2-integrinfrom Membrane Rafts to Caveolae and Subsequent Protein Kinase C-dependent Internalization. *Mol. Biol. Cell* **15**, 625–636.

Valdembri, D., Caswell, P. T., Anderson, K. I., Schwarz, J. P., König, I., Astanina, E., Caccavari, F., Norman, J. C., Humphries, M. J., Bussolino, F., et al. (2009). Neuropilin-1/GIPC1 signaling regulates alpha5beta1 integrin α2-integrintraffic and function in endothelial cells. *PLoS Biol.* **7**, e25.

Valdembri, D., Sandri, C., Santambrogio, M. and Serini, G. (2011). Regulation of integrins by conformation and traffic: it takes two to tango. *Mol Biosyst* **7**, 2539–46.

Vanneste, D., Takagi, M., Imamoto, N. and Vernos, I. (2009). The role of Hklp2 in the stabilization and maintenance of spindle bipolarity. *Curr. Biol.* **19**, 1712–7.

Veale, K. J., Offenhäuser, C., Whittaker, S. P., Estrella, R. P. and Murray, R. Z. (2010). Recycling endosome membrane incorporation into the leading edge regulates lamellipodia formation and macrophage migration. *Traffic* **11**, 1370–9.

Volpicelli-Daley, L. A., Li, Y., Zhang, C.-J. and Kahn, R. A. (2005). Isoform-selective effects of the depletion of ADP-ribosylation factors 1-5 on membrane traffic. *Mol. Biol. Cell* **16**, 4495–508.

Wang, J. and Howell, K. E. (2000). The luminal domain of TGN38 interacts with integrin α2-integrinbeta 1 and is involved in its trafficking. *Traffic* **1**, 713–23.

Winograd-Katz, S. E., Itzkovitz, S., Kam, Z. and Geiger, B. (2009). Multiparametric analysis of focal adhesion formation by RNAi-mediated gene knockdown. *J. Cell Biol.* **186**, 423–36.

Zhang, H., Berg, J. S., Li, Z., Wang, Y., Lång, P., Sousa, A. D., Bhaskar, A., Cheney, R. E. and Strömblad, S. (2004). Myosin-X provides a motor-based link between integrins and the cytoskeleton. *Nat. Cell Biol.* **6**, 523–31.

Zhu, C., Zhao, J., Bibikova, M., Leverson, J. D., Bossy-Wetzel, E., Fan, J.-B., Abraham, R. T. and Jiang, W. (2005a). Functional analysis of human microtubule-based motor proteins, the kinesins and dyneins, in mitosis/cytokinesis using RNA interference. *Mol. Biol. Cell* **16**, 3187–99.

Zhu, C., Bossy-Wetzel, E. and Jiang, W. (2005b). Recruitment of MKLP1 to the spindle midzone/midbody by INCENP is essential for midbody formation and completion of cytokinesis in human cells. *Biochem. J.***389**, 373–81.

Zutter, M. M., Sun, H. and Santoro, S. A. (1998). Altered integrin α2-integrinexpression and the malignant phenotype: the contribution of multiple integrated integrin α2-integrinreceptors. *J Mammary Gland Biol Neoplasia* **3**, 191–200.

Author Contributions

A.E. and V.S. designed the project and wrote the manuscript, A.E., S.R., A.A. and H.E. performed experiments, B.K. and L.K. did statistical data evaluation, D.M. and R.R. did bioinformatics data analysis, R.E., T.L., J.I. and R.P. contributed to the data interpretation.

Figure Legends

Fig. 1. Endocytic trafficking of endogenous α2-integrin in HeLa cells. Visualization of internalized (**A**), surface non-clustered (**B**) and antibody-clustered α2-integrin **(C)**. Quantification of the internalized (**D**) and cell surface α2-integrin (**E**). The amount of the internalized α2-integrin at the time point 1h and surface α2-integrin at the time point 0h was set to 100% (Y axis) in (**D**) and (**E**), respectively. Intracellular accumulation of α2-integrin is clathrin and caveolin dependent in HeLa cells **(F, G).** Scale bar in (**A,B,C,F**) = 20 µm. Error bars represent s.e.m. derived from three independent experiments in (**D, E, G**). * $p < 0,05$, ** $p < 0,01$, *** $p < 0,001$ (see Methods).

Fig. 2. **Co-localization of intracellular α2-integrin to Rab GTPases.** Endogenous α2-integrin (red) was co-localized to the over-expressed GFP-tagged Rab5a (**A**), mCherry-tagged Rab11b (**B**), GFP-tagged Rab4a (**C**), and GFP-tagged Rab7a (**D**) (green) 1h after the internalization. Thick arrows show co-localizing structures and arrowheads show not co-localizing structures in overlay images. Thin arrows show perinuclear localization of the over-expressed Rabs. Scale bar = 10 µm and scale bar of inserts = 5 µm.

Fig. 3. **Fluorescent microscopy-based screen identifies potential regulators of α2-integrin endocytic trafficking.** (**A**) Distribution of z-scores of 386 tested genes in the primary screen (z-scores of the most effective siRNA is shown for every gene, z-scores of other siRNAs are shown in

the **Supplementary Table 2**). Strong hits (z-scores > +/- 1,5) are listed, weak hits (z-score < +/- 1.5) are shown in green and non-effectors (z-score < +/-1) are shown in blue. (**B**) Examples of intracellular accumulation of α2-integrin specific fluorescence on cell arrays. White circles indicate spot boundaries within which α2-integrin specific fluorescence was measured. Scale bar = 100 μm. (**C**) Comparison of potential regulators of α2-integrin intracellular accumulation and the regulators of transferrin and EGF endocytosis (left graph), regulators of focal adhesion formation and epithelial cell migration (right graph).

Fig. 4. Validation of KIF15 role in α2-integrin endocytic trafficking. (**A**) Depletion of KIF15 by RNAi prevents appearance of intracellular α2-integrin and this effect is lessened by the over-expression of GFP-tagged KIF15, but not GFP. Asterisks indicate cells expressing high levels of GFP and GFP-tagged KIF15. (**B**) Quantification of the rescue of α2-integrin trafficking inhibition. (**C**) Biotin-capture ELISA based assay and quenching antibody based assay (**D**) show that α2-integrin and β1 intracellular accumulation, respectively, is inhibited when KIF15 is down-regulated. *, p≤0,05, ** p≤0,01, *** p≤0,001. Downregulation of KIF15 does not have influence on microtubules (**E**) and actin (**F**). Scale bar = 20 μm.

Fig. 5. **KIF15 is specifically required for the internalization of α2-integrin**. Downregulation of KIF15 inhibits internalization of α2-integrin (**A**), but internalization of transferrin (**B**) and EGF (**C**) is not affected. In difference, recycling of transferrin to PM is strongly inhibited (**B**). Scale bar = 20 μm. Quantification of α2-integrin (**D**), transferrin (**E**) and EGF (**F**) endocytic trafficking. Lines represent averaged intracellular intensities of each cargo, normalized to negative controls after 60 min of internalization of α2-integrin and 15 min of internalization of transferrin and EGF. Error bars indicate s.e.m. obtained from three independent experiments. *, p≤0,05.

Fig. 6. Depletion of CLASPs inhibits α2-integrin intracellular accumulation. Downregulation of Dab2 and ARH prevents α2-integrin intracellular accumulation (**A, B**), whereas, downregulation of Numb has no effect (**B**). (**C**) Downregulation efficiency of Dab2 as shown by WB. (**D**) Downregulation of mRNAs encoding Dab2, Numb and ARH as tested by qRT-PCR. Scale bar = 20 μm in (**A**). *, p≤0,05, ** p≤0,01.

Fig. 7. **KIF15 downregulation redistributes Dab2 from the PM. (A)** Downregulation of KIF15 displaces Dab2 associated with the PM (TIRF imaging mode) to the intracellular space (epifluorescence imaging mode, Epi). Epifluorescence and TIRF images are overlaid and dashed line indicates the position that was used for fluorescence intensity profile plotting. (**B**) Quantification of Dab2 specific mean fluorescent intensities imaged in Epi and TIRF modes. N = 15; error bars indicate s.e.m; *, p≤0,05. **(C)** Fluorescence intensity profile plot, showing Dab2 specific structures by TIRF and Epi modes. Arrows indicate Dab2 specific structures that are redistributed from the PM. Position (X axis) indicates a distance from the left end of the dashed line in (**A**). (**D**) KIF15 downregulation leads to loss of peripheral (indicated by arrowheads) and appearance of perinuclear localization of Dab2 (indicated by arrows) as visualized by confocal microscopy. 160 cells transfected with the negative control and 200 cells transfected with siRNAs targeting KIF15 were analysed. Scale bar = 20 µm.

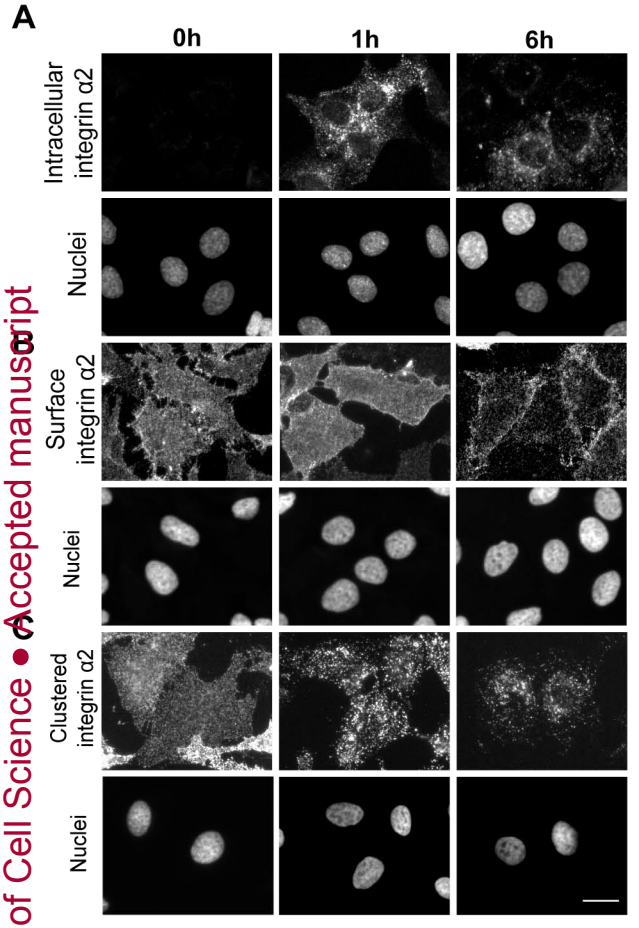

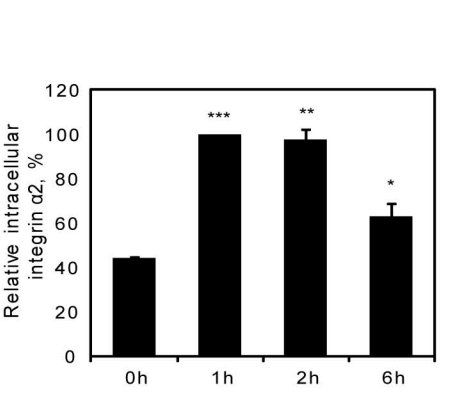

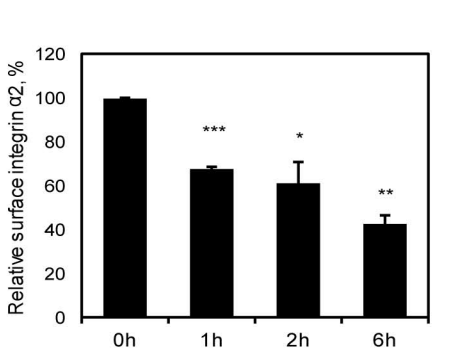

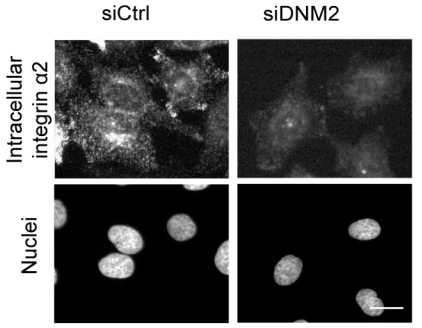

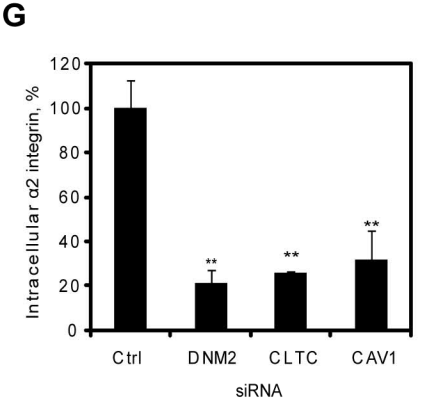

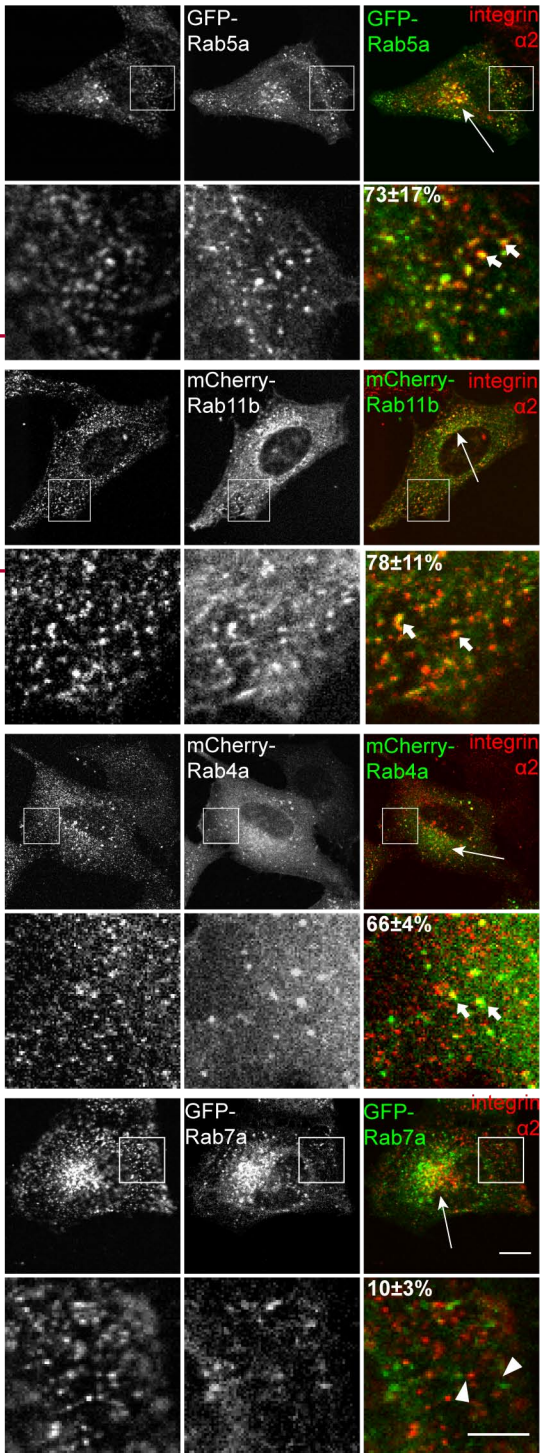

A

Strong inhibitors	
Gene Name	Z-score
SRGAP3	-2,24
PTEN	-2,23
ITGB3BP	-2,11
ARHGAP6	-2,11
DOCK5	-2,02
KIF1B	-1,99
PTPN11	-1,86
SDC4	-1,78
KIF18A	-1,76
CAPN1	-1,75
ARHGAP39	-1,74
MYO1D	-1,70
RND2	-1,69

FGD6	-1,64
PIK3CA	-1,64
KIF16B	-1,64
ARF1	-1,62
TRPM7	-1,61
MYO1A	-1,59
PTPN1	-1,57
PLEKHG6	-1,55
MYO18A	-1,55
LIMS1	-1,54
ACTN1	-1,53
MYO5A	-1,52
EZR	-1,51

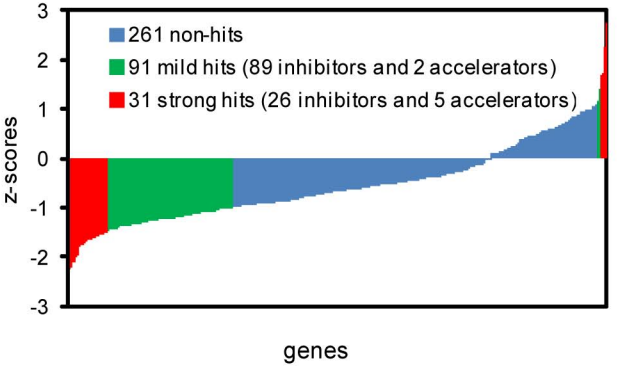

Strong accelerators	
Gene Name	Z-score
MCF2L2	1,53
ARHGEF38	1,70
NUDT16L1	1,73
ASAP1	2,27
CHN1	2,74

B

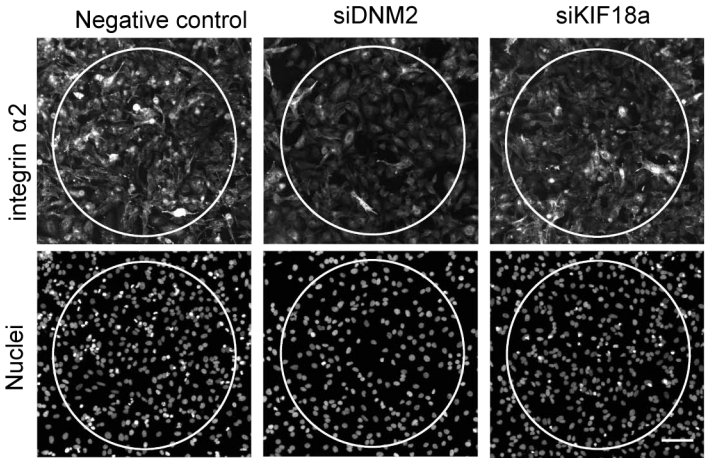

C

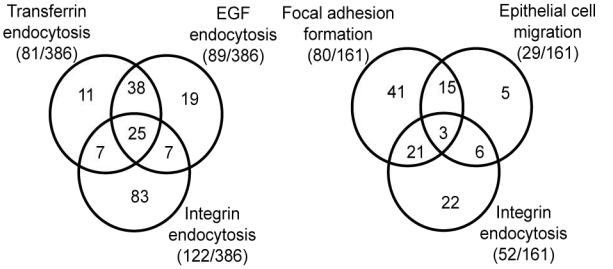

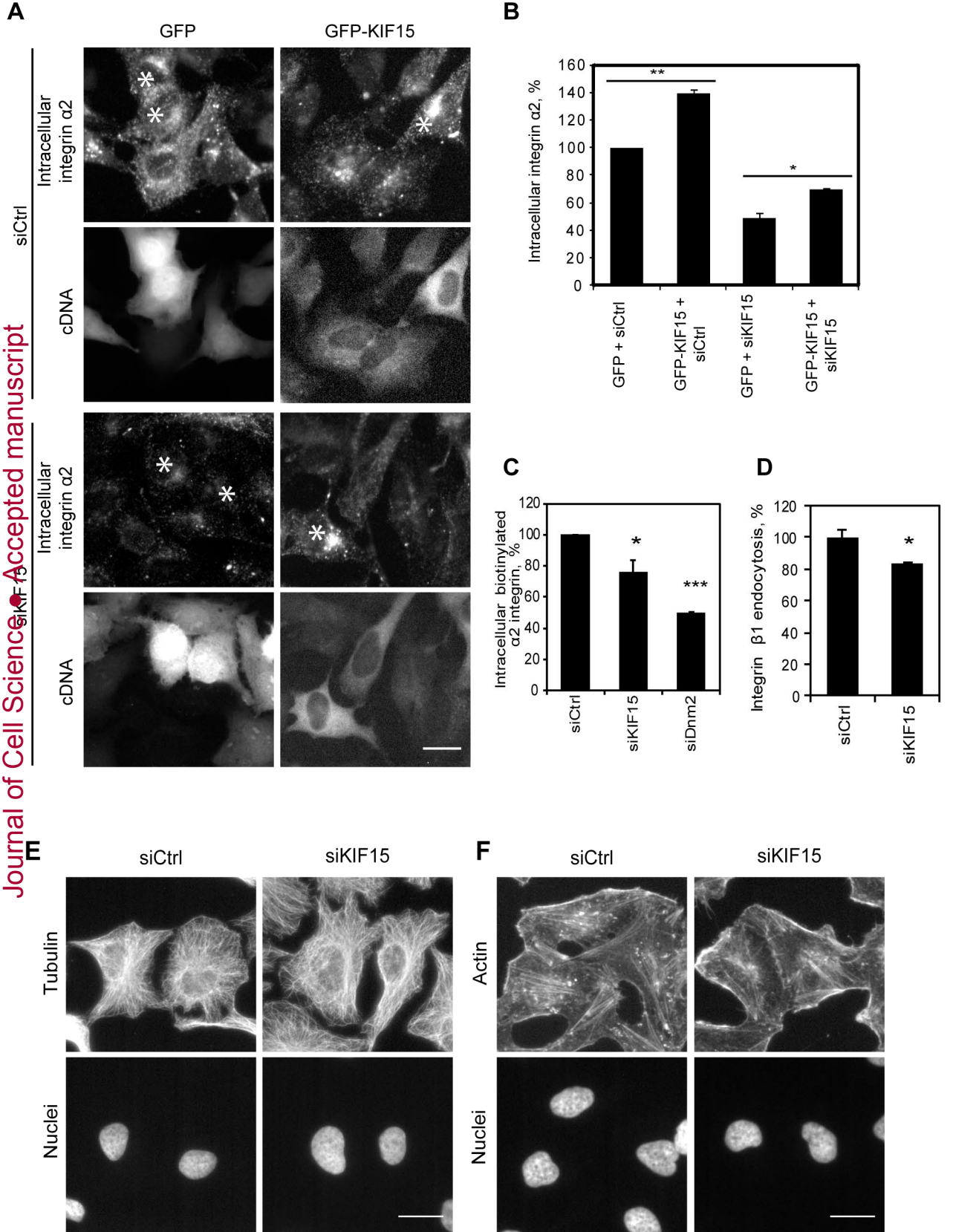

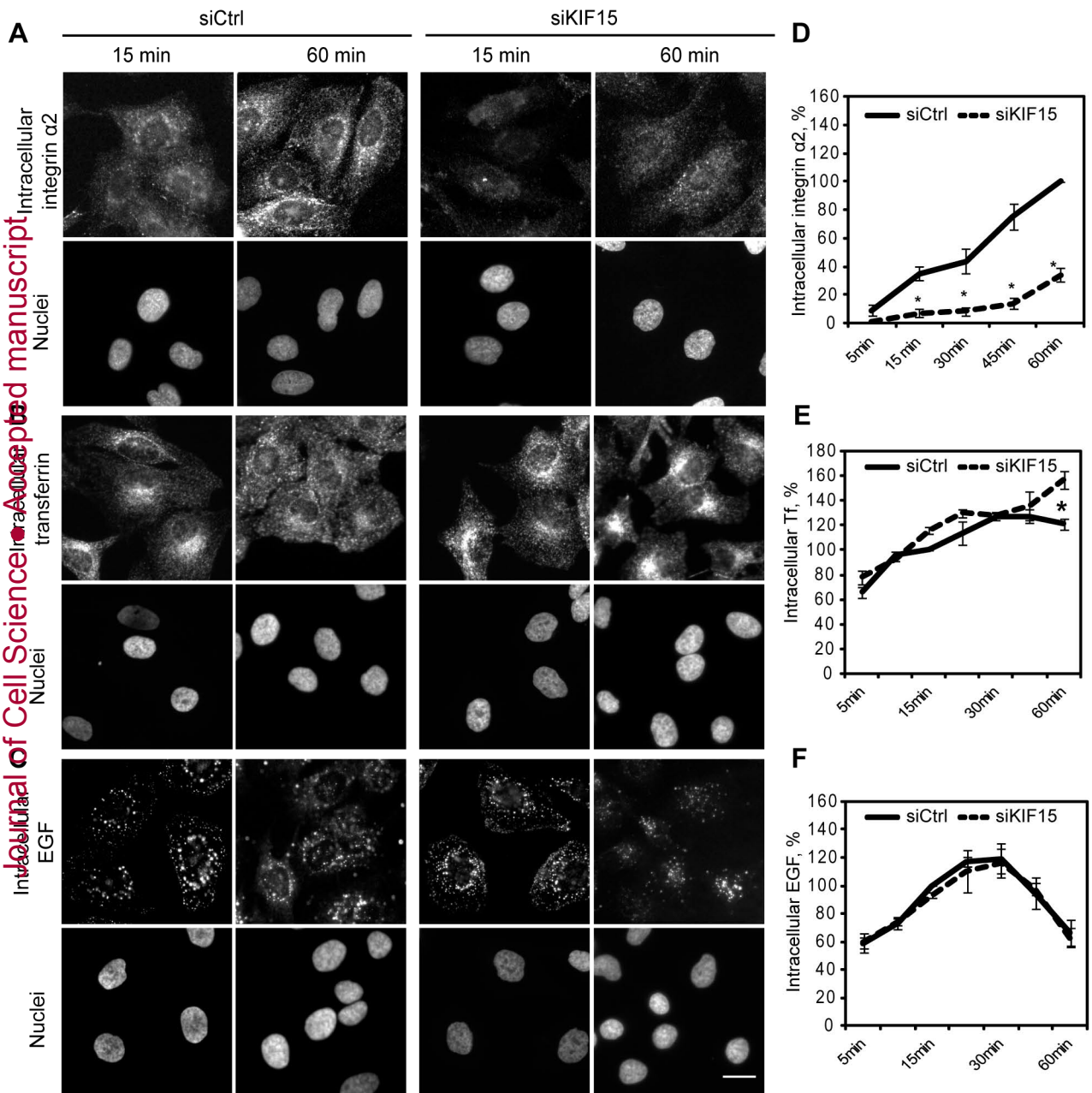

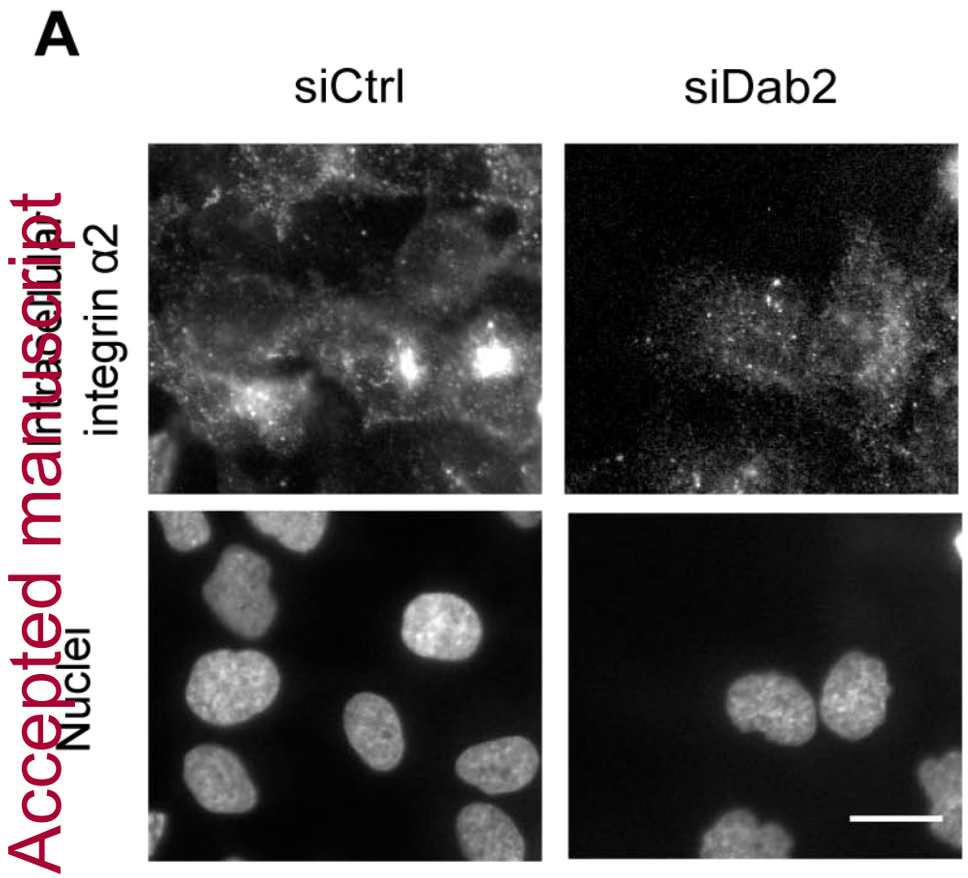

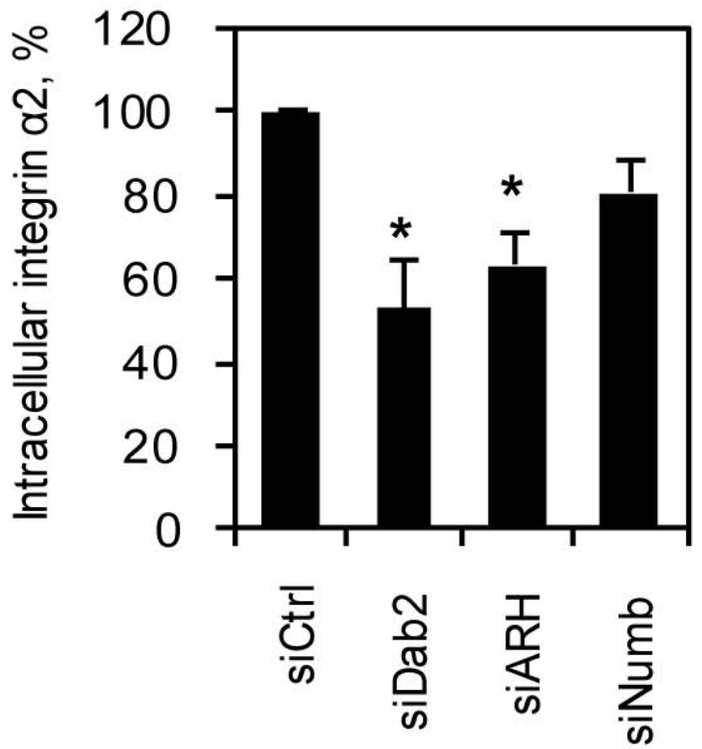

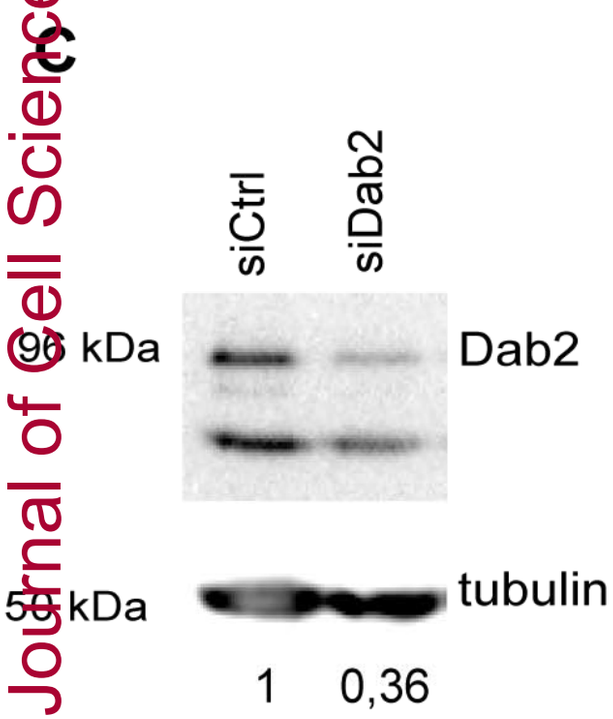

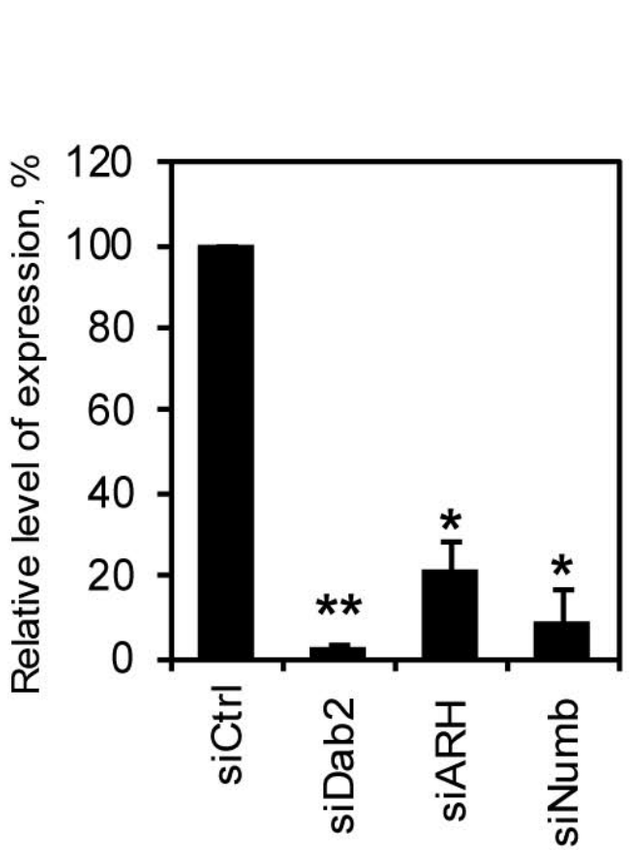

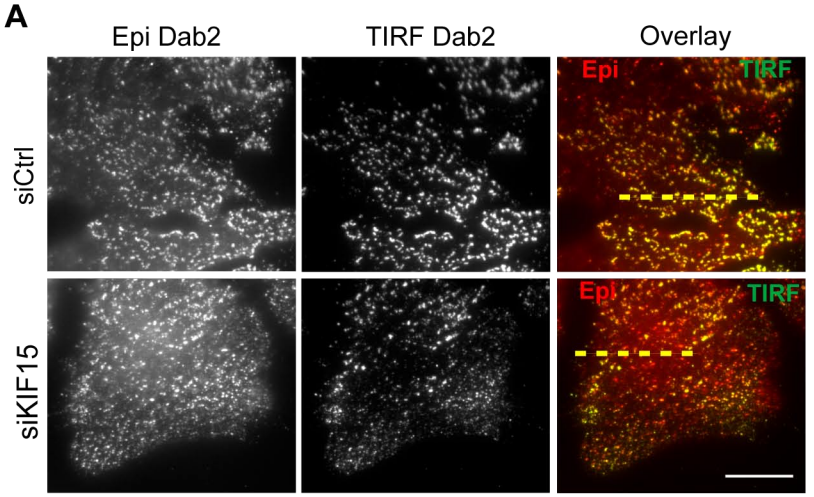

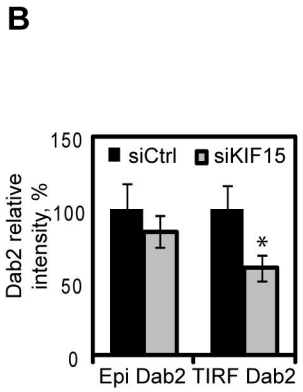

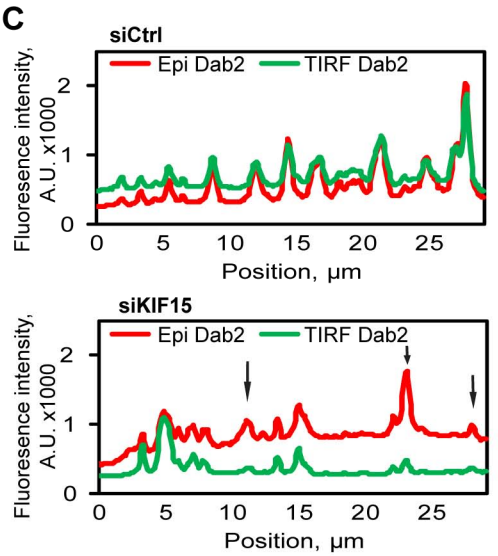

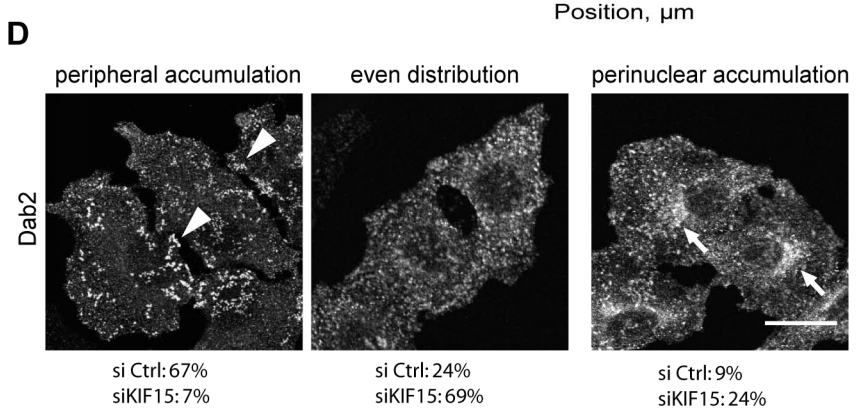

Table 1. **Validated regulators of α2-integrin intracellular accumulation**.

Gene name	Intracellular α2-integrin, %	Total α2-integrin, %	Cell count, %
Negative control	100	100	100
DNM2	27,2 ± 6,63	82,45 ± 13,77	98,56 ± 6,88
ARF1	49,17 ± 7,43	99,11 ± 17,67	99,16 ± 37,85
ABL2	52,78 ± 9,94	56,84 ± 4,49	72,05 ± 18,6
ARHGAP6	42,03 ± 6,35	43,14 ± 4,33	75,59 ± 7,24
ITGB1	7,38 ± 3,4	54,12 ± 7,1	99,93 ± 17,32
KIF15	27,8 ± 4,45	96,5 ± 2,3	106,44 ± 7,75
KIF18A	51,12 ± 9,54	97,64 ± 16,74	98,64 ± 31,44
KIF23	25,4 ± 6,36	92,69 ± 33,23	49,11 ± 22,74
Myo1A	36.43 ± 17.79	64,72 ± 4.04	126,42 ± 46,71
NF2	35,59 ± 3,1	95,89 ± 13,64	85,77 ± 3,19
PTPN11	39,11 ± 5,19	76,83 ± 3,72	66,07 ± 28,1

Validated regulators that inhibit α2-integrin intracellular accumulation without changing α2-integrin expression are shown in bold. Intracellular and total levels of α2-integrin represents average values (± S.E.M) of α2-integrin specific fluorescence derived from cells showing efficient endocytosis and all cells, respectively.